Analysis of friction and instability by the centre manifold theory for a non-linear sprag-slip model

Jean-Jacques Sinou, Fabrice Thouverez, Louis Jezequel

Journal home page : http://www.sciencedirect.com/science/journal/0022460X

Analysis of friction and instability by the centre manifold theory for a non-linear sprag-slip model
Journal of Sound and Vibration, Volume 265, Issue 3, 14 August 2003, Pages 527-559
J. -J. Sinou, F. Thouverez and L. Jezequel

ANALYSIS OF FRICTION AND INSTABILITY BY THE CENTER MANIFOLD THEORY FOR A NON-LINEAR SPRAG-SLIP MODEL.

J-J. SINOU * , F. THOUVEREZ and L. JEZEQUEL.

Laboratoire de Tribologie et Dynamique des Systèmes UMR CNRS 5513
Ecole Centrale de Lyon,69134 Ecully, France, *36 avenue Guy de Collongue, 69134 Ecully, France.*

ABSTRACT

This paper presents a research devoted to the study of instability phenomena in non-linear model with a constant brake friction coefficient. Indeed, the impact of unstable oscillation can be catastrophic. It can cause vehicle control problems and component degradation. Accordingly, complex stability analysis is required. This paper outlines stability analysis and center manifold approach for studying instability problem. To put it more precisely, one considers brake vibrations and more specifically heavy trucks judder where the dynamic characteristics of the whole front axle assembly is concerned, even if the source of judder is located in the brake system. The modelling introduces the sprag-slip mechanism based on dynamic coupling due to buttressing. The non-linearity is expressed as a polynomial with quadratic and cubic terms. This model does not require the use of brake negative coefficient, in order to predict the instability phenomena. Finally, the center manifold approach is used to obtain equations for the limit cycle amplitudes. The center manifold theory allows the reduction of the number of equations of the original system in order to obtain a simplified system, without loosing the dynamics of the original system as well as the contributions of non-linear terms. The goal is the study of the stability analysis and the validation of the center manifold approach for a complex non-linear model by comparing results obtained by solving the full system and by using the center manifold approach. The brake friction coefficient is used as an unfolding parameter of the fundamental Hopf bifurcation point.

1 INTRODUCTION

During the recent years, the understanding of the dynamic behaviour of systems with non-linear phenomena have been developed in order to predict dangerous or favourable conditions and to exploit the whole capability of structures by using system in the non-linear range. As an illustration, self-excited vibrations can have consequences, ranging from passenger discomfort, through reduced service life, to loss of control and catastrophe. Consequently, the customers' requests induce to consider the optimization of all elements of structure, and the dynamic design of products becomes one of the most important factors for manufacturers. Usually, a parametric study with linear stability theory is carried out to determine the effect of system parameters on stability. Stability was investigated by determining eigenvalues of the linearized perturbation equations about each steady-state operating point, or by calculating the Jacobian of the system at the equilibrium points. While stability analyses are extremely useful in evaluating the effect of changes in various system parameters, they cannot evaluate limit cycles amplitudes.

Of course, robust softwares have been developed in order to solve differential-algebraic equations corresponding to systems including several nonlinearities; time history response solutions of the full set of non-linear equations can determine the vibration amplitude. Nevertheless, the study of an instability problem may require consideration of several factors. In some cases, changes in masses, stiffnesses, or geometry, are necessary in order to stabilise a system; in other cases, vibration absorbers may be appropriate. In this way, time history response solutions of the full set of non-linear equations are both time consuming and costly to perform, when extensive parametric design studies are needed. For this reason, an understanding of the behaviour of systems with many degrees of freedom requires simplification methods in order to reduce the order of the system of equations and/or eliminate as many nonlinearities as possible in the system of equations. Moreover, many physical systems are modeled by differential equations depending on a control parameter. In the study of the dynamical behavior of such systems, bifurcation problems often arise within the control parameter range.

Due to the fact that such non-linear systems occur in many disciplines of engineering and science, considerable work has been devoted to effect explicit reductions. Perturbation methods, such as the methods of multiple scales and averaging (Nayfeh and Mook [1]), have been used as simplification methods in many studies. There is a reduction in the dimension, as one goes from the original system to the averaged system. The normal form approach can be also used to eliminate as many non-linear terms of the non-linear equations as possible through a non-linear change of variable. These problems have already been studied by several groups (Nayfeh and Balachandran [2], Brjuno [3]-[4], Guckhenheimer and Holmes [5], Jezequel and Lamarque [6], Iooss [7]-[8], Hsu [9]-[10], Yu [11], etc.). Moreover, one of the most important simplification method is the center manifold approach. The center manifold theorem (Marsden and McCracken [12]) characterises the local bifurcation analysis in the vicinity of a fixed point of the non-linear system. The center manifold approach can be compared as a simplification method that reduces the number of equations of the original system in order to obtain a simplified system without loosing the dynamics of the original system as well as the contributions of non-linear terms (Nayfeh and Balachandran [2], Guckhenheimer and Holmes [5], Knobloch and Wiesenfeld [13]). However, if this technique has been applied in scientific areas such as engineering, it has received little attention in the field of friction induced vibration in braking system.

In this paper, one applied the center manifold reduction to a self-excited system with many-degree-of-freedom containing quadratic and cubic non-linear terms that characterises the modelling of heavy trucks judder.

Firstly, some basic concepts of friction and brake noise will be introduced. Next, a model for the analysis of judder mode vibration in automobile braking systems will be presented. The model does not use brake negative damping and predicts that system instability can occur with a constant brake friction coefficient. Then, results from stability analyses and parametric studies using this model will be presented. System stability can be altered by changes in the brake friction coefficient, pressure, stiffness, geometry and various brake design parameters.

Finally, one will use the center manifold approach in order to predict limit cycle amplitudes. One proposes a compromise between an analytical method and a numerical approach in order to obtain limit cycles amplitudes. Usually, the polynomial approximations of stable variables as a power series in center manifold are obtained numerically. In this paper, one presents an analytical development for the calculation of the expression of second-order and third-order polynomial. Results from center manifold approach will be compared with results obtained by integrating the full original system in order to validate the center manifold approach and the polynomial approximations of stable variables as a power series in center variables.

2 FRICTION INDUCED BRAKE VIBRATION

A greater concentration of work on the brake noise and vibrations appeared during the last years. However there has been no uniformly accepted theory to characterise the problem; various types of vibrations have been investigated, such as disk brake squeal (North [14], Earles and Soar

[15] and Millner [16]), aircraft brake squeal (S.Y. Liu [17]), railway wheel squeal (Rudd [18]) and band brake squeal (Nakai [19]). In this way, analytical models have been proposed for the description of the dynamics of brake systems, including brake calliper, pads and disc: some of the most famous studies were proposed by Jarvis and Mill [20] (cantilever-disc models), Earles and Soar [15], Earles and Lee [21] (pin-disc models), Spurr [22] (sprag-slip model) and North [14] (binary flutter model).

One of the most important phases in studying the brake systems is the determination of the mechanism of the unstable friction induced vibration in brake systems. There is no unique mathematical model and theory in order to explain the mechanisms and dynamic phenomena associated with friction. According to Ibrahim [23]-[24], Oden and Martins[25], Crolla and Lang [26], there are four general mechanisms for friction-induced system instability, and more specifically friction-induced vibration in disc-brake systems: stick-slip, variable dynamic friction coefficient, sprag-slip and coupling mechanism.

The first two approaches rely on changes in the friction coefficient with relative sliding speed affecting the system stability. The last two approaches used kinematic constraints and modal coupling in order to develop the instability; in these cases, instability can occur with a constant brake friction coefficient.

Stick-slip is a low sliding speed phenomenon caused when the static friction coefficient is higher than the dynamic coefficient. A simple system that has been used for the examination of the stick-slip phenomenon is that of a mass sliding on a moving belt as shown in Figure 1(A). During the sliding phase, there is no change in the friction force that tends to make the mass stick on the moving belt. The sliding force increases until it exceeds the static friction force maximum. Consequently, the mass starts to slide. Next the mass continues to slide until the force causing the sliding drops to the sliding friction value. Then, sliding and sticking occur in succession.

Early in 1938, a study of Mills [27] led to an initial understanding that brake squeal was associated with a decrease in friction coefficient with rubbing speed as shown in Figure 1(A). Due to this negative slope, the steady state sliding becomes unstable and caused friction-induced vibrations. Although this mechanism is still recognised as explaining some low frequency brake vibration problems, it was soon realised that a decrease in friction coefficient was insufficient to explain some friction-induced vibrations.

Figure 1 : Stick-slip and sprag-slip models

It was later realised that this tribological property was not the only reason for a brake to squeal, and that vibration could occur when the friction coefficient remained sensibly constant with speed. Spurr [22] also proposed that instability with constant friction coefficient could occur by considering sprag-slip phenomenon. The sprag-slip phenomenon occurs due to locking action of the slider into the sliding surface as defined in Figure 1(B). An important failure of this mechanism is the angle α between the resulting force at the friction contact and the normal direction of the sliding belt.

Later, researchers gradually increased the sophistication of these sprag slip models by developing a more generalised theory describing the mechanism as a geometrically induced or kinematic constraint instability. At least two degrees of freedom are essential for this mechanism to be effective. For example, Jarvis and Mills [20] developed a cantilever-disc model in which the disc vibrated transversely due to spragging action. Their work showed that the variation of the coefficient of friction with sliding speed was insufficient to cause the friction-induced vibrations and so that the instability was due to coupling even if the coefficient of friction was constant. Modal coupling of the structure involved sliding parts and the coupling results in changes of friction forces necessary for self-excited vibration. In the same way, Earles [21], North [14], Miller [16], Dweib and D'Souza [28] described models using this latter theory for a single-pin-disc system and a double-pin-disc system, and showed that frictional instability can occur due to the coupling among the normal, tangential and torsional degrees of freedom. Some theoretical and experimental studies were investigated to shown that the stability was affected by varying the coefficient of friction, disc stiffness and geometry.

Actually, it is accepted that there is no uniformly theory for the characterisation of the problem and that stick-slip phenomenon (Larsson [29], Antoniou [30]), negative friction velocity slope (Black [31], Gao [32], etc), sprag-slip phenomenon and geometric coupling of the structure involving sliding parts (Boudot [33], Chambrette [34] and Moirot [35]) contributed to the description of mechanisms causing dynamic instability of the brake system.
Actually, the analysis of mechanism of disc brakes still presents a broad problem in spite of the numerous recent studies on the subject. Effectively, there are many types of brake vibration problem with various phenomena. It is clear that these headings can be described by using the same mechanism, even if a specificity, particularly experimental observations, exists for each group. Specialists as Crolla and Lang [15] divided them into three headings : disc brake noise, brake judder and brake drum noise.

Generally, brake noises are divided into categories according to the sound frequency. On the basis of previous brake experiments, there are many types of brake noises with varying phenomena as squeal noise, groan noise, jerder noise, squelch noise, pinch-out noise. Squeal noise and groan noise are the two important phenomena of brake noise. Technically speaking, noise is the result of a self-excited oscillation or dynamic instability of the brake. Squeal is accepted as being the result of such instabilities. For example, squeal can be due to a resonance of drums, rotors or back plates. The frequency spectrum of squeal is in the 1–10 kHz range. In contrast to squeal, groan occurs at very slow vehicle speed and, is caused by stick-slip at the rubbing surface; the frequency spectrum of groan is in the 10–300 Hz range.
The most important drum brake noise is squeal. As drum brakes were gradually replaced by disc brakes on vehicle front axles, studies and experimental investigations were gradually decreased. According to Kusamo [36], the drum brake noise frequency increased with increasing brake hydraulic pressure; moreover Lang [37] proposed introduction of asymmetry into drum structure in order to reduce drum brake squeal. The frequency spectrum of drum brake noise is observed in the 500–4000 Hz range.
Unlike brake noise, judder is a lower frequency vibration that is generally felt rather that heard. Judder is defined as a forced vibration. In order to find a solution to this friction-induced vibration and to minimize vibration, the effect of suspension and vehicle body dynamics on the transmission of judder to the driver have been investigated. The frequency spectrum of judder vibration is in the 10 – 100 Hz range.

3 ANALYTICAL MODEL

In order to link the effect of specific parameter variation on stability to the design features of brake system, it is necessary to work with mechanical models. Most of the analytical approaches can be divided into three parts. First, a parameter model including friction forces at the rubbing surface and mechanisms for friction induced system instability is established and the equations of motion are determined. Next, stability analyses are investigated by considering the parameter values that make the model stable or unstable. Finally, parametric studies are realised in order to relate the effect of specific parameter variation to the stability and to the evolution of limit cycle amplitudes. Indeed, changes in masses, stiffnesses, brake friction characteristics, damping, or geometry could be significant on stability. Various researchers successfully achieved the two first points (Earles and Chambers [38], Chambrette [34], Boudot [33] and Moirot [35]), but the effects of parameter variations were not always conducted; this is probably due to the fact that the determination of the vibration amplitude is both time consuming and costly to perform, when extensive parametric design studies are needed. So, these studies related only on the effect of parameter variations to stability, and neglected the studies of evolution of limit cycle amplitudes. One of the most important stages in the study of brake systems is the determination of parametric model.
In a previous work [33], Boudot presented heavy trucks judder. According to experimental investigations, judder vibration was observed on brake control and front axle assembly, and the frequency spectrum was in the 50–100 Hz range. It seems, therefore, that the dynamic characteristics of the whole front axle assembly is concerned, even if the source of judder is located

in the braking system. Moreover there is only a very small variation of the brake friction coefficient during a judder vibration event, as described by Boudot [32]. So the variation of the brake friction coefficient can be assumed to be negligible in this case, although this is not always the case for modelling brake systems. This context is selected because it is complex, both in order to be qualitatively predictive, and simple in order to allow sensitivity analysis. In this study, the mechanism used in order to explain the judder is a classical mechanism: brake judder is modelled as a flutter instability due to the non-conservative aspect of Coulomb's friction (Boudot [32], Chambrette[33] and Moirot [34]).
As a result, one considers the sprag-slip theory based on dynamic coupling due to buttressing; the dynamic characteristics of the front axle assembly will be concerned in judder vibration.
The dynamic system is defined in Figure 2 with the following assumptions:

- the brake friction coefficient μ is assumed to be a constant when brake vibrations occur.
- when the rotor is in rotating condition, the direction of the friction forces at the interface does not change.
- the speed V is constant and represents the rotation of the rotor.
- the rotor and the pad friction surfaces are always in contact.

Figure 2 : Dynamic model of braking system

Judder is a relatively complex self-excited vibration. It results from coupling between the torsional mode of the front axle and the normal mode of the brake control. In this way, the dynamic behaviour of the braking system is expressed by two free-free modes of the structure: the first (k_2, m_2) is tangential to the friction contact and the second (k_1, m_1) is normal to the friction contact. In the case of the grabbing of brake system, k_2 and m_2 define the torsional mode of the front axle excited by the tangential forces of the disc. The normal forces are provided by the brake control, whose dynamic behaviour is described by the second mode (k_1, m_1). Consequently, tangential and normal degree-of-freedom are coupled only by friction forces. This expresses the braking system contribution.
In order to simulate braking system placed crosswise due to overhanging caused by static force effect, one considers the moving belt slopes with an angle θ. This slope couples the normal and tangential degree-of-freedom induced only by the brake friction coefficient. This consideration called sprag-slip, is based on dynamic coupling due to buttressing motion. Moreover, one considers the effect of braking force, that is an important parameter in friction-induced vibration. The force F_{brake} transits through the braking command, that has non-linear behaviour. The dynamic system is modelled here as a three-degrees –of-freedom system: translational and normal displacement in the x-direction of the mass m_2 defined by $X(t)$ and $y(t)$, respectively, and the translational displacement in the y-direction of the mass m_1 defined by $Y(t)$.
Therefore, one considers the possibility of having a non-linear contribution. Then, one expresses this non-linear stiffness as a quadratic and cubic polynomial in the relative displacement:

$$\begin{aligned} k_1 &= k_{11} + k_{12}.\Delta + k_{13}.\Delta^2 \\ k_2 &= k_{21} + k_{22}.\delta + k_{23}.\delta^2 \end{aligned} \tag{1}$$

where Δ is the relative displacement between the normal displacement in the y-direction of the mass m_1 and the mass m_2 (one has $\Delta = y - Y$), and δ the translational displacement defined by the frictional x-direction of the mass m_2 (one has $\delta = X$). This nonlinearity is applied in order to indicate the influence and the importance of non-linear terms in the understanding of the dynamic behaviour of systems with non-linear phenomena, the prediction of dangerous or favourable conditions, and the exploitation of the full capability of structures by using system in the non-linear range. To be more precise, the non-linear behaviour dynamic of the brake command of the system (k_1, m_1), and the non-linear behaviour dynamic of the front axle assembly and the suspension (k_2, m_2) are concerned, respectively.

One assumes that the tangential force T is generated by the brake friction coefficient μ, considering the Coulomb's friction law:

$$T = \mu.N \tag{2}$$

With reference to figure 2, and considering the non-linear expression of the stiffness k_2 defined in equation (1), the equation of motion in the Ox-direction for the mass m_2 can be written as

$$m_2\ddot{X} + c_2\dot{X} + k_{21}X + k_{22}X^2 + k_{23}X^3 = -N\sin\theta + T\cos\theta \tag{3}$$

Considering the non-linear expression of the stiffness k_1 defined in equation (1), the equation of motion in the Oy-direction for the mass m_2 can be written as

$$m_2\ddot{y} + c_1(\dot{y} - \dot{Y}) + k_{11}(y - Y) + k_{12}(y - Y)^2 + k_{13}(y - Y)^3 = N\cos\theta + T\sin\theta \tag{4}$$

and the equation of motion in the Oy-direction for the mass m_1 as

$$m_1\ddot{Y} + c_1(\dot{Y} - \dot{y}) + k_{11}(Y - y) + k_{12}(Y - y)^2 + k_{13}(Y - y)^3 = -F_{brake} \tag{5}$$

Finally, the three equations of motion can be expressed as

$$\begin{cases} m_1\ddot{Y} + c_1(\dot{Y} - \dot{y}) + k_{11}(Y - y) + k_{12}(Y - y)^2 + k_{13}(Y - y)^3 = -F_{brake} \\ m_2\ddot{X} + c_2\dot{X} + k_{21}X + k_{22}X^2 + k_{23}X^3 = -N\sin\theta + T\cos\theta \\ m_2\ddot{y} + c_1(\dot{y} - \dot{Y}) + k_{11}(y - Y) + k_{12}(y - Y)^2 + k_{13}(y - Y)^3 = N\cos\theta + T\sin\theta \end{cases} \tag{6}$$

Using the transformations $y = X\tan\theta$ and $\mathbf{x} = \{X \;\; Y\}^{\mathrm{T}}$, and considering the Coulomb's friction law $T = \mu.N$, the non-linear *2*-degrees-of-freedom system has the form

$$\mathbf{M}.\ddot{\mathbf{x}} + \mathbf{C}.\dot{\mathbf{x}} + \mathbf{K}.\mathbf{x} = \mathbf{F} + \mathbf{F_{NL}} \tag{7}$$

where $\ddot{\mathbf{x}}$, $\dot{\mathbf{x}}$ and $\mathbf{x}$ are the acceleration, velocity, and displacement response 2-dimensional vectors of the degrees-of-freedom, respectively. $\mathbf{M}$ is the mass matrix, $\mathbf{C}$ is the damping matrix and $\mathbf{K}$ is the stiffness matrix. $\mathbf{F}$ is the vector force due to brake command and $\mathbf{F_{NL}}$ contains moreover the non-linear stiffness terms. One has

$$\mathbf{M} = \begin{bmatrix} m_2\left(\tan^2\theta + 1\right) & 0 \\ 0 & m_1 \end{bmatrix} \tag{8}$$

$$\mathbf{C} = \begin{bmatrix} c_1\left(\tan^2\theta - \mu\tan\theta\right) + c_2\left(1 + \mu\tan\theta\right) & c_1\left(-\tan\theta + \mu\right) \\ -c_1\tan\theta & c_1 \end{bmatrix} \tag{9}$$

$$\mathbf{K} = \begin{bmatrix} k_{21}\left(1 + \mu\tan\theta\right) + k_{11}\left(\tan^2\theta - \mu\tan\theta\right) & k_{11}\left(-\tan\theta + \mu\right) \\ -k_{11}\tan\theta & k_{11} \end{bmatrix} \tag{10}$$

$$\mathbf{F_{NL}} = \begin{Bmatrix} \left(-\tan\theta + \mu\right)\left(k_{12}\left(X\tan\theta - Y\right)^2 + k_{13}\left(X\tan\theta - Y\right)^3\right) + k_{22}\left(1 + \mu\tan\theta\right)X^2 + k_{23}\left(1 + \mu\tan\theta\right)X^3 \\ -k_{12}\left(Y - X\tan\theta\right)^2 - k_{13}\left(Y - X\tan\theta\right)^3 \end{Bmatrix} \tag{11}$$

$$\mathbf{F} = \begin{Bmatrix} 0 \\ -F_{brake} \end{Bmatrix} \tag{12}$$

The values of the parameters are given in Appendix A.

The general form of the equation of motion for the non-linear judder model can be expressed in the following way:

$$\mathbf{M}.\ddot{\mathbf{x}} + \mathbf{C}.\dot{\mathbf{x}} + \mathbf{K}.\mathbf{x} = \mathbf{F} + \sum_{i=1}^{n}\sum_{j=1}^{n} \mathbf{f}_{(2)}^{\mathbf{ij}} . x_i . x_j + \sum_{i=1}^{n}\sum_{j=1}^{n}\sum_{k=1}^{n} \mathbf{f}_{(3)}^{\mathbf{ijk}} . x_i . x_j . x_k \tag{13}$$

where $\mathbf{f}_{(2)}^{\mathbf{ij}}$ and $\mathbf{f}_{(3)}^{\mathbf{ijk}}$ are the vectors of quadratic and cubic non-linear terms, respectively. $\mathbf{M}$, $\mathbf{C}$ and $\mathbf{K}$ are 2×2 matrices.

4 SOLUTION METHODOLOGY

The study can be divided in two parts. The first one is the static problem: the steady state operating point for the full set of non-linear equations is obtained by their solving at the equilibrium point. Stability is investigated by calculating the Jacobian of the system at the equilibrium points. The second step is the estimation of the limit cycle. The non-linear dynamic equations can be integrated numerically in order to obtain a time-history response and the limit cycle. However this procedure is too much time consuming. So the equations are reduced by the center manifold theory. This approach simplifies the dynamics on the center manifold by the reduction of the order of the dynamical system; however it retains the essential features of the dynamic behaviour near the Hopf bifurcation point.

The first step in the solution procedure is to obtain the steady –state-operating point for the full set of the non-linear sprag-slip equations (13) by the determination of the equilibrium point. The equilibrium point $\mathbf{x_0}$ is obtained by solving the non-linear static equations for a given net brake hydraulic pressure. This equilibrium point satisfies the following conditions:

$$\mathbf{K}.\mathbf{x_0} = \mathbf{F} + \mathbf{F_{NL}}(\mathbf{x_0}) \tag{14}$$

One notes that there can be more than one steady-state operating point at a given net brake hydraulic pressure, since the sprag-slip equations are non-linear.

The stability is investigated by calculating the Jacobian of the system at the equilibrium points. The complete expression of the Jacobian matrix $\mathbf{J}$ is given in Appendix B. The eigenvalues of the constant matrix $\mathbf{J}$ provide information about the local stability of the equilibrium point $\mathbf{x_0}$. Moreover, it is possible to obtain the 4th-degree characteristic polynomial

$$\lambda^4 + a_3\lambda^3 + a_2\lambda^2 + a_1\lambda + a_0 = 0 \tag{15}$$

where λ are the eigenvalues of the Jacobian matrix $\mathbf{J}$. The expressions of a_3, a_2, a_1 and a_0 are given in Appendix B. We note that this polynomial defines the 4th-degree characteristic polynomial of the linearized system.

If all roots of the characteristic equation (15) have a negative real part, the system is stable and one does not have vibration. If one root has a positive real part, one has an unstable root and vibration. The imaginary part of this root represents the frequency of the unstable mode. Moreover, applying the Routh-Hurwitz criterion [39] to this characteristic equation gives the following conditions for the stability : (a) $a_3 > 0$; (b) $a_2a_3 - a_1 > 0$; (c) $a_1(a_2a_3 - a_1) - a_0{a_3}^2 > 0$.

Using the base parameters defined previously, the computations are conducted with respect to the brake friction coefficient. The Hopf bifurcation point is detected for $\mu_0 = 0{,}2$.

A representation of the evolution of frequencies against brake friction coefficient is given in Figure 3. In Figure 4, the associated real parts are plotted. As shown in Figure 3, one notices that there are two stable modes at different frequencies when $\mu < \mu_0$. On the other hand, the real part of eigenvalues is negative when $\mu < \mu_0$ as illustrated in Figure 4. As the brake friction coefficient increases, these two modes move closer until they reach the bifurcation zone. One obtains the

coalescence for $\mu = \mu_0$ of two imaginary parts of the eigenvalues (frequency about 50 Hz). For $\mu = \mu_0$, there is one pair of purely imaginary eigenvalues. All other eigenvalues have negative real parts. After the bifurcation, the two modes couple and form a complex pair as shown in Figure 3. On the other hand, the real part of eigenvalues is positive as illustrated in Figure 4.

As showed in Figure 3, the system is unstable for $\mu > \mu_0$, and stable for $\mu < \mu_0$. This stability analysis indicates that the instability can occur with a constant friction coefficient. Moreover, the frequency ω_0 of the unstable mode, obtained for $\mu = \mu_0$ is near 50 Hz. There is a perfect correlation with experiment tests where judder vibration is observed in the 40-70 Hz range.

Figure 3 : Coupling of two eigenvalues

Figure 4 : Evolution of the real part of two coupling modes

Moreover, it is possible to perform a stability analysis using two parameters. There is obviously an infinity of combinations of parameters that could be examined. The base parameters are taken as the starting set for this investigation. The evolutions of stable and unstable regions versus two specific parameters are shown in Figure 5a-Figure 12a. With regard to the evolution of coupled resonant frequency, a simple representation can be obtained by plotting frequency and the real part of eigenvalue on the complex plan as illustrated in Figure 5b-Figure 12b. The vertical axis shows the frequency and the horizontal axis is a measurement of system damping. The right side of the complex plan is the unstable region, where modes have negative damping. Conversely, the left side of the complex plan is the stable region, where modes are uncoupled. One knows that the modes couple and form a complex pair after the Hopf bifurcation. In fact, the range coupled resonance frequency is determined at the bifurcation point $\mu = \mu_0$.

It is observed that stability is a complex problem. Parametric design studies show that stability can be altered by changes in the brake friction coefficient, brake force, stiffness, damping and angle. Some general indications have been obtained. It must be emphasized that increasing or decreasing stiffness, angle and mass have some effect on the stable region. This is further reflected in Figure 5-Figure 12.

To put it more precisely, decreasing brake friction coefficient reduces unstable region. In some case, as illustrated in Figure 8, Figure 9 and Figure 11, the two-coupled modes can reach the bifurcation zone and decoupled by decreasing brake friction coefficient. This is one way to stabilise the system.

On the other hand, parametric studies as a function of angle θ and stiffness k_{21} or as a function of angle θ and stiffness k_{21} are very interesting. Indeed, in this case, one observes a closed unstable region as shown in Figure 10. This close area is readily explained by the evolution of modes that coupled and decoupled with the evolution of parameters. For example, in Figure 10, the modes reach the bifurcation zone at $k_{21} \approx 0{,}75e5N/m$ for $\theta = 0.15rad$ and coupled when $k_{21} \geq 0{,}75e5N/m$. But, the two modes reach again the bifurcation zone at $k_{21} \approx 1{,}25e5N/m$ for $\theta = 0.15rad$ and decoupled when $k_{21} \leq 1{,}25e5N/m$. So, one has successively stable, unstable and stable zones for $\theta = 0.15rad$ with varying stiffness coefficient k_{21}.

Moreover, decreasing both linear stiffness k_{11} and k_{21} reduces the unstable region as illustrated in Figure 7. The frequency spectrum of resonant coupled vibration is in the 10–70 Hz range.

The angle θ is also very important in the stabilization the system, as shown in Figure 8 and Figure 10. For the purposes of comparison, stability as a function of stiffness k_{11} and brake friction coefficient (Figure 11), and stability as a function of stiffness k_{21} and brake friction coefficient (Figure 9), are similar. However, one can note that unstable regions show some small differences versus the stiffnesses.

Consequently, a stability study is a very complex problem: stable and unstable regions can be obtained by varying parameters and one has an infinity of combinations of parameters that could be examined. As an example of possible parametric studies, Figure 5 to Figure 12 illustrated stability

analysis and the frequency range of resonant coupled vibration. In some cases, stable and unstable zones are very simple; in other cases, more complex zones of instability can be obtained.

Figure 5 : Stability and complex eigenvalues as a function of mass m_1 and stiffness k_{11}. Coupled resonant frequencies between 47-57 Hz.

Figure 6 : Stability and complex eigenvalues as a function of force F_{brake} and stiffness k_{11}. Coupled resonant frequencies between 47-48 Hz and 55-56 Hz.

Figure 7: Stability and complex eigenvalues as a function of stiffness k_{21} and stiffness k_{11}. Coupled resonant frequencies between 10-70 Hz.

Figure 8 : Stability and complex eigenvalues as a function of angle θ and brake friction coefficient. Coupled resonant frequencies between 50-51 Hz.

Figure 9 : Stability and complex eigenvalues as a function of stiffness k_{21} and brake friction coefficient. Coupled resonant frequencies between 45-58 Hz.

Figure 10 : Stability and complex eigenvalues as a function of angle θ and stiffness k_{21}. Coupled resonant frequencies between 47-54 Hz.

Figure 11 : Stability and complex eigenvalues as a function of stiffness k_{11} and brake friction coefficient. Coupled resonant frequencies between 48-52 Hz.

Figure 12 : Stability and complex eigenvalues as a function of stiffness k_{12} and force F_{brake}. Coupled resonant frequencies between 47-47 Hz.

5 COMPLEX NONLINEAR PROBLEM

In order to conduct a complex non-linear analysis, it is necessary to consider complete expressions of the non-linear forces. Moreover, the complete non-linear expressions of the non-linear forces are expressed about the equilibrium point $\mathbf{x_0}$ for small perturbations $\bar{\mathbf{x}}$:

$$\mathbf{x} = \mathbf{x_0} + \bar{\mathbf{x}} \tag{16}$$

The complete non-linear equation can be written as follow:

$$\mathbf{M}.\ddot{\bar{\mathbf{x}}} + \mathbf{C}.\dot{\bar{\mathbf{x}}} + \mathbf{K}.\bar{\mathbf{x}} = \mathbf{P_{NL}}\left(\bar{\mathbf{x}}\right) \tag{17}$$

where $\ddot{\bar{\mathbf{x}}}$, $\dot{\bar{\mathbf{x}}}$ and $\bar{\mathbf{x}}$ are the acceleration, velocity, and displacement response two-dimensional vectors of the degrees-of-freedom, respectively. $\mathbf{M}$ is the mass matrix, $\mathbf{C}$ is the damping matrix and $\mathbf{K}$ is the stiffness matrix. $\mathbf{P_{NL}} = \left\{P_{NL}^X \quad P_{NL}^Y\right\}^{\mathrm{T}}$ is the non-linear force due to net brake hydraulic pressure and non-linear stiffness. It contains the linear and non-linear terms about the equilibrium point for small perturbations. One has:

$$P_{NL}^X = F_L^X + F_{NL}^X \tag{18}$$

$$P_{NL}^Y = F_L^Y + F_{NL}^Y \tag{19}$$

where F_L^X , F_L^Y are the linear terms of P_{NL}^X and P_{NL}^Y . F_{NL}^X and F_{NL}^Y are the quadratic and cubic terms of P_{NL}^X and P_{NL}^Y about the equilibrium point. These expressions are:

$$\begin{aligned} F_L^X\left(\bar{\mathbf{x}}\right) = \left(-\tan\theta + \mu\right)\Big[& 2k_{12}\tan^2\theta.X_0.\bar{X} + 2k_{12}.Y_0.\bar{Y} - 2k_{12}\tan\theta.Y_0.\bar{X} - 2k_{12}\tan\theta.X_0.\bar{Y} \\ & + 3k_{13}\tan^3\theta.{X_0}^2.\bar{X} - 6k_{13}\tan^2\theta.X_0.Y_0.\bar{X} - 3k_{13}\tan^2\theta.{X_0}^2.\bar{Y} + 3k_{13}\tan\theta.{Y_0}^2.\bar{X} \\ & + 6k_{13}\tan\theta.X_0.Y_0.\bar{Y} - 3k_{13}.{Y_0}^2.\bar{Y}\Big] + \left(1 + \mu\tan\theta\right)\Big[2k_{22}.X_0.\bar{X} + 3k_{23}.{X_0}^2.\bar{X}\Big] \end{aligned} \tag{20}$$

$$F_L^Y(\bar{\mathbf{x}}) = -2k_{12}.Y_0.\bar{Y} - 2k_{12}\tan^2\theta.X_0.\bar{X} + 2k_{12}\tan\theta.X_0.\bar{Y} + 2k_{12}\tan\theta.Y_0.\bar{X} \\ -3k_{13}.Y_0^2.\bar{Y} + 6k_{13}\tan\theta.X_0.Y_0.\bar{Y} + 3k_{13}\tan\theta.Y_0^2.\bar{X} \\ -3k_{13}\tan^2\theta.X_0^2.\bar{Y} - 6k_{13}\tan^2\theta.X_0.Y_0.\bar{X} + 3k_{13}\tan^3\theta.X_0^2.\bar{X} \tag{21}$$

$$F_{NL}^X(\bar{\mathbf{x}}) = k_{12}.(-\tan\theta+\mu).\left[\tan^2\theta.\bar{X}^2 + \bar{Y}^2 - 2\tan\theta.\bar{X}\bar{Y}\right] + k_{13}.(-\tan\theta+\mu).\left[\tan^3\theta.\left(\bar{X}^3 + 3\bar{X}^2X_0\right)\right. \\ -3\tan^2\theta.\left(\bar{X}^2\bar{Y} + 2\bar{X}\bar{Y}X_0 + \bar{X}^2X_0\right) + 3\tan\theta\left(\bar{X}\bar{Y}^2 + 2\bar{X}\bar{Y}Y_0 + \bar{Y}^2Y_0\right) - \bar{Y}^3 - 3\bar{Y}^2Y_0\left.\right] \\ +k_{22}.(1+\mu\tan\theta).\bar{X}^2 + k_{23}.(1+\mu\tan\theta).\left[\bar{X}^3 + 3\bar{X}^2X_0\right] \tag{22}$$

$$F_{NL}^Y(\bar{\mathbf{x}}) = k_{12}.\left[\bar{Y}^2 - 2\tan\theta.\bar{X}\bar{Y} + \tan^2\theta.\bar{X}^2\right] + k_{13}.\left(\bar{Y}^3 + 3\bar{Y}^2Y_0\right) - 3\tan\theta.\left(\bar{X}\bar{Y}^2 + 2\bar{X}\bar{Y}Y_0 + \bar{Y}^2X_0\right) \\ +3\tan^2\theta\left(\bar{X}^2\bar{Y} + 2\bar{X}\bar{Y}X_0 + \bar{X}^2Y_0\right) - \tan^3\theta.\left(\bar{X}^3 + 3\bar{X}^2Y_0\right) \tag{23}$$

The non-linear sprag-slip equation about the equilibrium point $\mathbf{x_0} = \{X_0 \;\; Y_0\}^{\mathrm{T}}$ for small perturbations $\bar{\mathbf{x}} = \{\bar{X} \;\; \bar{Y}\}^{\mathrm{T}}$ can be expressed as

$$\mathbf{M}.\ddot{\bar{\mathbf{x}}} + \mathbf{C}.\dot{\bar{\mathbf{x}}} + \mathbf{K}.\bar{\mathbf{x}} = \sum_{i=1}^{2}\mathbf{f_{(1)}^{i}}.\bar{x}_i + \sum_{i=1}^{2}\sum_{j=1}^{2}\mathbf{f_{(2)}^{ij}}.\bar{x}_i.\bar{x}_j + \sum_{i=1}^{2}\sum_{j=1}^{2}\sum_{k=1}^{2}\mathbf{f_{(3)}^{ijk}}.\bar{x}_i.\bar{x}_j.\bar{x}_k \tag{24}$$

where the vectors $\mathbf{f_{(1)}^{i}}$, $\mathbf{f_{(2)}^{ij}}$ and $\mathbf{f_{(3)}^{ijk}}$ are the coefficients of the linear, quadratic and cubic terms due to the non-linear stiffness about the equilibrium point, respectively.
The rearrangement of the linear and non-linear terms on the left and right sides of equation (24), respectively, gives the new non-linear system

$$\mathbf{M}.\ddot{\bar{\mathbf{x}}} + \mathbf{C}.\dot{\bar{\mathbf{x}}} + \tilde{\mathbf{K}}.\bar{\mathbf{x}} = \sum_{i=1}^{2}\sum_{j=1}^{2}\mathbf{f_{(2)}^{ij}}.\bar{x}_i.\bar{x}_j + \sum_{i=1}^{2}\sum_{j=1}^{2}\sum_{k=1}^{2}\mathbf{f_{(3)}^{ijk}}.\bar{x}_i.\bar{x}_j.\bar{x}_k \tag{25}$$

One notes that $\tilde{\mathbf{K}}$ is the stiffness matrix containing the terms of the first stiffness matrix $\mathbf{K}$ defined in equation (10), and the linear terms F_L^X and F_L^Y of P_{NL}^X and F_{NL}^Y about the equilibrium point defined in equations (20) and (21), respectively. The vectors $\mathbf{f_{(2)}^{ij}}$ and $\mathbf{f_{(3)}^{ijk}}$ are the coefficients of the quadratic and cubic terms, respectively, due to the non-linear stiffness about the equilibrium point. The expressions of $\mathbf{f_{(1)}^{i}}$, $\mathbf{f_{(2)}^{ij}}$ and $\mathbf{f_{(3)}^{ijk}}$ are given in Appendix C.
In order to obtain time-history responses, the complete set of non-linear dynamic equations may be integrated numerically. However this procedure is time consuming, when parametric design studies are needed. So one will present the center manifold approach in order to obtain equations for the limit cycle amplitude.
In order to use the center manifold approach, the non-linear judder equation is written in state variables

$$\dot{\mathbf{y}} = \mathbf{A}.\mathbf{y} + \sum_{i=1}^{2n}\sum_{j=1}^{2n}\boldsymbol{\eta}_{\mathbf{(2)}}^{\mathbf{ij}}.y_i.y_j + \sum_{i=1}^{2n}\sum_{j=1}^{2n}\sum_{k=1}^{2n}\boldsymbol{\eta}_{\mathbf{(3)}}^{\mathbf{ijk}}.y_i.y_j.y_k \tag{26}$$

where

$$\mathbf{y} = \begin{Bmatrix}\bar{\mathbf{x}} \\ \dot{\bar{\mathbf{x}}}\end{Bmatrix} \tag{27}$$

$$\dot{\mathbf{y}} = \begin{Bmatrix}\dot{\bar{\mathbf{x}}} \\ \ddot{\bar{\mathbf{x}}}\end{Bmatrix} \tag{28}$$

$$\mathbf{A} = -\begin{bmatrix} \mathbf{C} & \mathbf{M} \\ \mathbf{I} & \mathbf{0} \end{bmatrix}^{-1} \cdot \begin{bmatrix} \widetilde{\mathbf{K}} & \mathbf{0} \\ \mathbf{0} & \mathbf{I} \end{bmatrix} \tag{29}$$

$$\boldsymbol{\eta}_{(2)} = \begin{bmatrix} \mathbf{C} & \mathbf{M} \\ \mathbf{I} & \mathbf{0} \end{bmatrix}^{-1} \cdot \begin{bmatrix} \mathbf{f}_{(2)} \\ \mathbf{0} \end{bmatrix} \tag{30}$$

$$\boldsymbol{\eta}_{(3)} = \begin{bmatrix} \mathbf{C} & \mathbf{M} \\ \mathbf{I} & \mathbf{0} \end{bmatrix}^{-1} \cdot \begin{bmatrix} \mathbf{f}_{(3)} \\ \mathbf{0} \end{bmatrix} \tag{31}$$

$\boldsymbol{\eta}_{(2)}^{\mathbf{ij}}$ and $\boldsymbol{\eta}_{(3)}^{\mathbf{ijk}}$ are quadratic and cubic non-linear terms of the state variables, respectively.
This system can be written by using the Kronecker product $\otimes$ (Stewart [40]):

$$\dot{\mathbf{y}} = \mathbf{A}.\mathbf{y} + \boldsymbol{\eta}_{(2)}.\mathbf{y} \otimes \mathbf{y} + \boldsymbol{\eta}_{(3)}.\mathbf{y} \otimes \mathbf{y} \otimes \mathbf{y} \tag{32}$$

where $\mathbf{y} \otimes \mathbf{y}$ is defined as the basis of quadratic terms and $\mathbf{y} \otimes \mathbf{y} \otimes \mathbf{y}$ is defined as the basis of cubic terms. $\mathbf{A}$ is a 4×4 matrix.

6 THE CENTER MANIFOLD APPROACH

In this section, one describes the method to obtain the lower dimensional system, defined on the center manifold. Locally, the stability of the center manifold is equivalent to the stability of the original system.
One considers the non-linear ordinary 4 dimensionnal differential equations

$$\dot{\mathbf{y}} = \mathbf{f}(\mathbf{y}, \mu) = \mathbf{A}(\mu).\mathbf{y} + + \boldsymbol{\eta}_{(2)}.\mathbf{y} \otimes \mathbf{y} + \boldsymbol{\eta}_{(3)}.\mathbf{y} \otimes \mathbf{y} \otimes \mathbf{y} \tag{33}$$

where μ is a parameter. $\mathbf{A}(\mu)$, $\boldsymbol{\eta}_{(2)}^{\mathbf{ij}}$ and $\boldsymbol{\eta}_{(3)}^{\mathbf{ijk}}$ are the 4×4 matrix, quadratic and cubic non-linear terms, respectively, evaluated at the equilibrium point and defined previously in equations (30) and (31). This system has an equilibrium point $\mathbf{X_0}(\mu)$ if $\mathbf{f}(\mathbf{X_0}, \mu) = \mathbf{0}$. One may assume, without loss of generality, that $\mathbf{X_0} = \mathbf{0}$. The stability of this point is obtained by the analysis of eigenvalues of the linearized system. The bifurcation appears when one or several eigenvalues cross the imaginary axis in the complex plane with the variation of μ.
At the Hopf bifurcation point, the previous system can be written in the form

$$\begin{cases} \dot{\mathbf{v}}_\mathbf{c} = \mathbf{J_c}.\mathbf{v_c} + \mathbf{G_2}(\mathbf{v_c}, \mathbf{v_s}) + \mathbf{G_3}(\mathbf{v_c}, \mathbf{v_s}) \\ \dot{\mathbf{v}}_\mathbf{s} = \mathbf{J_s}.\mathbf{v_s} + \mathbf{H_2}(\mathbf{v_c}, \mathbf{v_s}) + \mathbf{H_3}(\mathbf{v_c}, \mathbf{v_s}) \end{cases} \tag{34}$$

where $\mathbf{J_c}$ and $\mathbf{J_s}$ have eigenvalues λ such as $Re[\lambda_{\mathbf{Jc}}(\mu_0)] = 0$ and $Re[\lambda_{\mathbf{Js}}(\mu_0)] \neq 0$. $\mathbf{G_2}, \mathbf{G_3}, \mathbf{H_2}$ and $\mathbf{H_3}$ are polynomials of degree 2 and 3 in the components of $\mathbf{v_c}$ and $\mathbf{v_s}$. By considering the physically interesting case of the stable equilibrium loosing stability, it may assume that all eigenvalues of $\mathbf{J_s}$ have negative real part. Moreover, one considers the first coupling modes. For a Hopf bifurcation, the center variables is two-dimensional. Consequently, $\mathbf{v_c}$ is consists of two terms $\mathbf{v_c} = \{v_{c1} \;\; v_{c2}\}^{\mathrm{T}}$. Because $\mathbf{G_2}, \mathbf{G_3}, \mathbf{H_2}$ and $\mathbf{H_3}$ are polynomials of degree 2 and 3 in the components of $\mathbf{v_c}$ and $\mathbf{v_s}$, they are infinitely differentiable. So, a local center manifold exists and the center manifold theory allows the expression of the variables $\mathbf{v_s}$ as a function of $\mathbf{v_c}$ (Carr [41], 1981):

$$\mathbf{v_s} = \mathbf{h}(\mathbf{v_c}) \tag{35}$$

It is very important to note that $\mathbf{v_s}$ is a local invariant manifold, since the expression of $\mathbf{v_s}$ as a function of $\mathbf{v_c}$ satisfies equation (34) for only small $\|\mathbf{v_c}\|$. The expression of $\mathbf{h}$ cannot be solved explicitly. However, it is possible to define an approximate solution of $\mathbf{h}$ by a power expansion. Considering the tangency conditions at the bifurcation point to the center eigenspace, the function $\mathbf{h}$ satisfied to $\mathbf{h}(\mathbf{0})=\mathbf{0}$ and $D\mathbf{h}(\mathbf{0})=\mathbf{0}$; the polynomial approximations do not contain constant and linear terms. One defines $\mathbf{v_s}=\mathbf{h}(\mathbf{v_c})$ as a power series in $\mathbf{v_c}$ of degree m, without constant and linear terms ($m \geq 2$).

Upon differentiating equation (35) and substituting into the second equation of equations (34) one obtains

$$D_{\mathbf{v_c}}\left(\mathbf{h}(\mathbf{v_c})\right).\left(\mathbf{J_c}.\mathbf{v_c}+\mathbf{G_2}\left[\mathbf{v_c},\mathbf{h}(\mathbf{v_c})\right]+\mathbf{G_3}\left[\mathbf{v_c},\mathbf{h}(\mathbf{v_c})\right]\right)=\mathbf{J_s}.\mathbf{h}(\mathbf{v_c})+\mathbf{H_2}\left[\mathbf{v_c},\mathbf{h}(\mathbf{v_c})\right]+\mathbf{H_3}\left[\mathbf{v_c},\mathbf{h}(\mathbf{v_c})\right] \quad (36)$$

By solving of equation (36), one obtains the coefficients of the terms of $\mathbf{h}$. Provided that a polynomial approximation of $\mathbf{h}$ up to sufficient order is obtained, the dynamics of equation (33) restricted to the center manifold is defined by the system:

$$\dot{\mathbf{v}}_\mathbf{c}=\mathbf{J_c}.\mathbf{v_c}+\mathbf{G_2}\left(\mathbf{v_c},\mathbf{h}\left(\mathbf{v_c}\right)\right)+\mathbf{G_3}\left(\mathbf{v_c},\mathbf{h}\left(\mathbf{v_c}\right)\right) \quad (37)$$

where $\mathbf{G_2}$ and $\mathbf{G_3}$ are given as a power series in $\mathbf{v_c}$ for the parameter $\mu=\mu_0$. $\mathbf{v_s}=\mathbf{h}(\mathbf{v_c})$ is a power series in $\mathbf{v_c}$ of degree m, without constant and linear terms ($m \geq 2$).

The stability of this reduced system is equivalent to that of the original system. Here one reduces the number of equation from 4 to 2. Moreover, the more complex the non-linear system is and has a lot of degree-of-freedom, the more interesting the center manifold approach is, allowing to save time.

In this study, one will consider a simple extension to the center manifold method when dealing with parametrized system. The final stage involves a consideration of the dynamics for parameter values near the bifurcation point. An extension of the center manifold theorem to the system (34) is the consideration of the augmented system as

$$\begin{cases}\dot{\mathbf{v}}_\mathbf{c}=\mathbf{J_c}\left(\hat{\mu}\right).\mathbf{v_c}+\mathbf{G_2}\left(\mathbf{v_c},\mathbf{v_s},\hat{\mu}\right)+\mathbf{G_3}\left(\mathbf{v_c},\mathbf{v_s},\hat{\mu}\right)\\ \dot{\mathbf{v}}_\mathbf{s}=\mathbf{J_s}\left(\hat{\mu}\right).\mathbf{v_s}+\mathbf{H_2}\left(\mathbf{v_c},\mathbf{v_s},\hat{\mu}\right)+\mathbf{H_3}\left(\mathbf{v_c},\mathbf{v_s},\hat{\mu}\right)\\ \dot{\hat{\mu}}=0\end{cases} \quad (38)$$

where $\hat{\mu}$ is a parameter. At $\left(\mathbf{v_c},\mathbf{v_s},\hat{\mu}\right)=(\mathbf{0},\mathbf{0},0)$, this system has a 3-dimensional center manifold tangent to $\left(\mathbf{v_c},\hat{\mu}\right)$ space. For small $\|\mathbf{v_c}\|$ and $\|\hat{\mu}\|$, the center manifold is described by

$$\mathbf{v_s}=\mathbf{h}\left(\mathbf{v_c},\hat{\mu}\right) \quad (39)$$

where the function $\mathbf{h}$ is such that, at the fixed point $(\mathbf{0},\mathbf{0},0)$,

$$\mathbf{h}=\mathbf{0},\ D\mathbf{h}(\mathbf{0})=\mathbf{0} \text{ and } \partial\mathbf{h}/\partial\hat{\mu}=0 \quad (40)$$

Therefore, the local center manifold is represented by the polynomial expansion of degree m

$$\mathbf{v_s}=\mathbf{h}\left(\mathbf{v_c},\hat{\mu}\right)=\sum_{p=i+j+l=2}^{m}\sum_{j=0}^{p}\sum_{l=0}^{p}\mathbf{a_{ijl}}.v_{c1}^{i}.v_{c2}^{j}.\hat{\mu}^{l} \quad (41)$$

where $\mathbf{a_{ijl}}$ are vectors of constant coefficients. One notices that the terms such as $v_{c1}\hat{\mu}$, $v_{c2}\hat{\mu}$, $v_{s1}\hat{\mu}$ and $v_{s2}\hat{\mu}$ are treated as nonlinear terms. The vectors $\mathbf{a_{ijl}}$ will be determined by solving the equation (36), augmented with the parameter $\hat{\mu}$. One obtains

$$\begin{aligned} &D_{\mathbf{v_c},\hat{\mu}}\left(\mathbf{h}\left(\mathbf{v_c},\hat{\mu}\right)\right).\left(\mathbf{J_c}.\mathbf{v_c}+\mathbf{G_2}\left[\mathbf{v_c},\mathbf{h}\left(\mathbf{v_c},\hat{\mu}\right),\hat{\mu}\right]+\mathbf{G_3}\left[\mathbf{v_c},\mathbf{h}\left(\mathbf{v_c},\hat{\mu}\right),\hat{\mu}\right]\right) \\ &=\mathbf{J_s}.\mathbf{h}\left(\mathbf{v_c},\hat{\mu}\right)+\mathbf{H_2}\left[\mathbf{v_c},\mathbf{h}\left(\mathbf{v_c},\hat{\mu}\right),\hat{\mu}\right]+\mathbf{H_3}\left[\mathbf{v_c},\mathbf{h}\left(\mathbf{v_c},\hat{\mu}\right),\hat{\mu}\right] \end{aligned} \tag{42}$$

Moreover, the dynamic of equation (33) restricted to the center manifold and augmented with the consideration of the parameter $\hat{\mu}$ is defined by the system:

$$\begin{cases} \dot{\mathbf{v}}_\mathbf{c}=\mathbf{J_c}\left(\hat{\mu}\right).\mathbf{v_c}+\mathbf{G_2}\left(\mathbf{v_c},\mathbf{h}\left(\mathbf{v_c},\hat{\mu}\right),\hat{\mu}\right)+\mathbf{G_3}\left(\mathbf{v_c},\mathbf{h}\left(\mathbf{v_c},\hat{\mu}\right),\hat{\mu}\right) \\ \dot{\hat{\mu}}=0 \end{cases} \tag{43}$$

7 DETERMINATION OF THE COEFFICIENTS

In order to obtain an approximation of the stable variables $\mathbf{v_s}$ as power series in $\left(\mathbf{v_c},\hat{\mu}\right)$, one may obtain the coefficients $a_{k,ijl}$ defined in equation (41). Usually, the polynomial approximations are taken as quadratic or cubic in the first approximation. But in studies of hard non-linear dynamical systems with more than 2-degree-of-freedom, the second-order or the third-order polynomial approximation is not sufficient to provide a good approximation of the stable and unstable variables. In fact, the fourth-order (or higher order) polynomial approximation is used in order to describe correctly the dynamics of the system. It is impossible to obtain an analytical expression of the coefficients $a_{k,ijl}$, due to the complexity of the polynomial approximations and the important numbers of non-linearities where the center, stable and unstable variables are nonlinearly coupled.

Now, it is possible to describe a systematic analytical method in order to perform the determination of the coefficients $a_{k,ijl}$, by using the increasing power of equations (42), and retaining only the terms corresponding to the power investigated. First, the developed expression of equation (34) has the form

$$\begin{cases} \dot{\mathbf{v}}_\mathbf{c}=\mathbf{J_c}.\mathbf{v_c}+G^{ij}_{(2)}.\mathbf{v}\otimes\mathbf{v}+G^{ik}_{(3)}.\mathbf{v}\otimes\mathbf{v}\otimes\mathbf{v} \\ \dot{\mathbf{v}}_\mathbf{s}=\mathbf{J_s}.\mathbf{v_s}+H^{ij}_{(2)}.\mathbf{v}\otimes\mathbf{v}+H^{ik}_{(3)}.\mathbf{v}\otimes\mathbf{v}\otimes\mathbf{v} \\ \dot{\hat{\mu}}=0 \end{cases} \tag{44}$$

with $\mathbf{v}=\left\{v_{c1}\quad v_{c2}\quad v_{s1}\quad v_{s2}\quad \hat{\mu}\right\}^T$. $G^{ij}_{(2)}, G^{ik}_{(3)}$, $H^{ij}_{(2)}$ and $H^{ik}_{(3)}$ are quadratic and cubic non-linear terms of $\mathbf{v}$, respectively (with $i=1,2$, $j=1,...,25$ and $k=1,...,125$). These notations will be used to defined expressions for the coefficients of the polynomial approximations $\mathbf{v_s}=\mathbf{h}(\mathbf{v_c},\hat{\mu})$ as a power series in $\left(\mathbf{v_c},\hat{\mu}\right)$.

7.1 SECOND-ORDER SOLUTION

One can express the stable variables by using second-order polynomial approximations. One recalls that the polynomial approximations contain no constant or linear terms. So, the expressions of the stable variables $\mathbf{v_s}$ as a power series in $\left(\mathbf{v_c},\hat{\mu}\right)$ of degree 2 can be written as

$$\begin{aligned}\mathbf{v_s} &= \mathbf{h^{(1)}}\left(\mathbf{v_c}, \hat{\mu}\right) = \sum_{p=i+j+l=2}^{2} \sum_{j=0}^{p} \sum_{l=0}^{p} \mathbf{a_{ijl}}.v_{c1}^{i}.v_{c2}^{j}.\hat{\mu}^{l} \\ &= \mathbf{a_{200}}.v_{c1}^{2} + \mathbf{a_{110}}.v_{c1}.v_{c2} + \mathbf{a_{020}}.v_{c2}^{2} + \mathbf{a_{101}}.v_{c1}.\hat{\mu} + \mathbf{a_{011}}.v_{c2}.\hat{\mu} + \mathbf{a_{002}}.\hat{\mu}^{2}\end{aligned} \tag{45}$$

where $\mathbf{a_{ijl}}$ are unknown vectors of coefficients. To find the $6\times n$ coefficients (where n defined the number of stable variables, $n=2$ in this case), one needs only the coefficients of the second-order terms in the polynomials on both sides in equations (36). So, by considering only second-order terms, the simplified expression of equation (36) has the form:

$$D_{\mathbf{v_c},\hat{\mu}}\left(\mathbf{h^{(1)}}\left(\mathbf{v_c}, \hat{\mu}\right)\right).\mathbf{J_c}.\mathbf{v_c} = \mathbf{J_s}.\mathbf{h^{(1)}}\left(\mathbf{v_c}, \hat{\mu}\right) + \mathbf{H_2}\left(\mathbf{v_c}, \hat{\mu}\right) \tag{46}$$

One notes that this system is the exact system for second-order polynomial approximations. It is possible to obtain an analytical expression of the coefficients $a_{k,ijl}$ by solving equation (46). One obtains

$$\begin{aligned} a_{k,200} &= \frac{H_{(2)}^{k1}}{2J_{c1} - J_{sk}} \quad ; \quad a_{k,110} = \frac{H_{(2)}^{k2} + H_{(2)}^{k6}}{J_{c1} + J_{c2} - J_{sk}} \quad ; \quad a_{k,020} = \frac{H_{(2)}^{k7}}{2J_{c2} - J_{sk}} \\ a_{k,101} &= \frac{H_{(2)}^{k5} + H_{(2)}^{k21}}{J_{c1} - J_{sk}} \quad ; \quad a_{k,011} = \frac{H_{(2)}^{k10} + H_{(2)}^{k22}}{J_{c2} - J_{sk}} \quad ; \quad a_{k,002} = \frac{-H_{(2)}^{k25}}{J_{sk}} \end{aligned} \tag{47}$$

For $k=1,2$. k defines the k^{th} degree-of-freedom of stable variables. J_{c1} and J_{c2} are the first and second terms of the diagonal matrix $\mathbf{J_c}$ as defined in equation (44), respectively. J_{sk} is the k^{th} term of the diagonal matrix $\mathbf{J_s}$ as defined in equation (44). $H_{(2)}^{ki}$ defined the term of the k^{th}-line and i^{th}-column of the matrix defined by $\mathbf{H_2}$. Now, one observes that the expression of the stable variables uses only the quadratic non-linear terms of center variables on the right side of equation (42) contained in $\mathbf{H_2}$. All quadratic terms of center variables on the left side of equation (42), as well as quadratic and cubic terms of stable variables on both sides, are not considered for the determination of the coefficients $a_{k,ijl}$.

Here, the second order approximation is not sufficient, due to the fact that the limit cycles obtained by integrating equation (43) diverge. Effectively, equations describing the dynamics of the system (33) on the center manifold, and described in equation (34), contain all linear, quadratic and cubic terms, but the dynamics of this reduced and of the original sytems , defined in equation (43), are not equivalent. The methodology and center manifold theory is not in question, but the polynomial approximation of stable variables $\mathbf{v_s}$ as a power series in $\left(\mathbf{v_c}, \hat{\mu}\right)$ of degree 2 does not represent a good approximation. So, it is necessary to define the third-order (or fourth-order, etc) polynomial approximation in order to describe correctly the dynamics of the system.

7.2 THIRD-ORDER SOLUTION

One has previously shown that the second-order polynomial approximation was not sufficient. So one needs to use the third-order polynomial approximation. The expressions of the stable variables $\mathbf{v_s}$, as a power series in $\left(\mathbf{v_c}, \hat{\mu}\right)$ of degree 3 without constant and linear terms, can be defined by adding third-order polynomial terms in the first second-order polynomial approximation defined in (45). These expressions have the form:

$$\begin{aligned}\mathbf{v_s} &= \sum_{p=i+j+l=2}^{3}\sum_{j=0}^{p}\sum_{l=0}^{p}\mathbf{a_{ijl}}.v_{c1}^{i}.v_{c2}^{j}.\hat{\mu}^{l} = \mathbf{h^{(1)}}\left(\mathbf{v_c},\hat{\mu}\right)+\mathbf{h^{(2)}}\left(\mathbf{v_c},\hat{\mu}\right)\\ &= \mathbf{h^{(1)}}\left(\mathbf{v_c},\hat{\mu}\right)+\mathbf{a_{300}}.v_{c1}^{3}+\mathbf{a_{210}}.v_{c1}^{2}.v_{c2}+\mathbf{a_{120}}.v_{c1}.v_{c2}^{2}+\mathbf{a_{030}}.v_{c2}^{3}\\ &+\mathbf{a_{201}}.v_{c1}^{2}.\hat{\mu}+\mathbf{a_{111}}.v_{c1}.v_{c2}.\hat{\mu}+\mathbf{a_{021}}.v_{c2}^{2}.\hat{\mu}+\mathbf{a_{102}}.v_{c1}.\hat{\mu}^{2}+\mathbf{a_{012}}.v_{c2}.\hat{\mu}^{2}+\mathbf{a_{003}}.\hat{\mu}^{3}\end{aligned} \tag{48}$$

where $\mathbf{a_{ijl}}$ are unknown vectors of coefficients (for $i+j+l=3$). $\mathbf{h^{(1)}}\left(\mathbf{v_c},\hat{\mu}\right)$ defines the first approximation using second-order polynomial approximation. In fact, substituting the assumed quadratic and cubic polynomial approximations in equation (42) and equating the coefficients of the different terms in the polynomials on both sides, gave the same system of algebraic equations for the coefficients of the polynomials, than that obtained by considering second-order and neglecting higher order. Therefore, one only needs to find the $10\times n$ coefficients (where n defined the number of stable variables, $n=2$ in this case) of the third-order terms in the polynomials on both sides in equations (42). So, the consideration of the third-order terms gives the simplified expression of equation (42):

$$\begin{aligned}&D_{\mathbf{v_c},\hat{\mu}}\left(\mathbf{h^{(1)}}\left(\mathbf{v_c},\hat{\mu}\right)\right).\left[\mathbf{G_2}\left(\mathbf{v_c},\hat{\mu}\right)\right].+D_{\mathbf{v_c}}\left(\mathbf{h^{(2)}}\left(\mathbf{v_c},\hat{\mu}\right)\right).\mathbf{J_c}.\mathbf{v_c}\\ &=\mathbf{J_s}.\mathbf{v_s}+\mathbf{H_2}\left(\left\{\mathbf{v_c},\mathbf{0},\hat{\mu}\right\}\otimes\left\{\mathbf{v_c},\mathbf{h^{(1)}}\left(\mathbf{v_c},\hat{\mu}\right),\hat{\mu}\right\}+\left\{\mathbf{0},\mathbf{h^{(1)}}\left(\mathbf{v_c},\hat{\mu}\right)\right\}\otimes\left\{\mathbf{v_c},\mathbf{0},\hat{\mu}\right\}\right)+\mathbf{H_3}\left(\mathbf{v_c},\hat{\mu}\right)\end{aligned} \tag{49}$$

This system is the exact system for third-order polynomial approximations. It is possible to obtain an analytical expression of the coefficients $a_{k,ijl}$ by solving equation (49). So, one obtains

$$a_{k,300}=\frac{-2a_{k,200}G_{(2)}^{11}+a_{1,200}\left(H_{(2)}^{k3}+H_{(2)}^{k11}\right)+a_{2,200}\left(H_{(2)}^{k4}+H_{(2)}^{k16}\right)-a_{k,110}G_{(2)}^{21}+H_{(3)}^{k1}}{3J_{c1}-J_{sk}}$$

$$a_{k,210}=\frac{\begin{array}{c}-2a_{k,200}\left(G_{(2)}^{12}+G_{(2)}^{16}\right)-a_{k,110}\left(G_{(2)}^{11}+G_{(2)}^{22}+G_{(2)}^{26}\right)-2a_{k,020}G_{(2)}^{21}+a_{1,110}\left(H_{(2)}^{k3}+H_{(2)}^{k11}\right)\\ +a_{2,110}\left(H_{(2)}^{k4}+H_{(2)}^{k16}\right)+a_{1,200}\left(H_{(2)}^{k8}+H_{(2)}^{k112}\right)+a_{2,200}\left(H_{(2)}^{k9}+H_{(2)}^{k117}\right)+H_{(3)}^{k2}+H_{(3)}^{k6}+H_{(3)}^{k26}\end{array}}{2J_{c1}+J_{c2}-J_{sk}}$$

$$a_{k,120}=\frac{\begin{array}{c}-2a_{k,200}G_{(2)}^{17}-a_{k,110}\left(G_{(2)}^{27}+G_{(2)}^{12}+G_{(2)}^{16}\right)-2a_{k,020}\left(G_{(2)}^{22}+G_{(2)}^{26}\right)+a_{1,020}\left(H_{(2)}^{k3}+H_{(2)}^{k11}\right)\\ +a_{2,020}\left(H_{(2)}^{k4}+H_{(2)}^{k16}\right)+a_{1,110}\left(H_{(2)}^{k8}+H_{(2)}^{k12}\right)+a_{2,110}\left(H_{(2)}^{k9}+H_{(2)}^{k17}\right)+H_{(3)}^{k7}+H_{(3)}^{k27}+H_{(3)}^{k31}\end{array}}{J_{c1}+2J_{c2}-J_{sk}}$$

$$a_{k,030}=\frac{-2a_{k,020}G_{(2)}^{27}+a_{1,020}\left(H_{(2)}^{k8}+H_{(2)}^{k12}\right)+a_{2,020}\left(H_{(2)}^{k9}+H_{(2)}^{k17}\right)-a_{k,110}G_{(2)}^{17}+H_{(3)}^{k32}}{3J_{c2}-J_{sk}}$$

$$a_{k,201}=\frac{\begin{array}{c}-a_{k,101}G_{(2)}^{11}-a_{k,011}G_{(2)}^{21}-2a_{k,200}\left(G_{(2)}^{15}+G_{(2)}^{121}\right)-a_{k,110}\left(G_{(2)}^{25}+G_{(2)}^{221}\right)+a_{1,101}\left(H_{(2)}^{k3}+H_{(2)}^{k11}\right)\\ +a_{2,101}\left(H_{(2)}^{k4}+H_{(2)}^{k16}\right)+a_{1,200}\left(H_{(2)}^{k15}+H_{(2)}^{k23}\right)+a_{2,200}\left(H_{(2)}^{k20}+H_{(2)}^{k24}\right)+H_{(3)}^{k5}+H_{(3)}^{k21}+H_{(3)}^{k101}\end{array}}{2J_{c1}-J_{sk}}$$

$$a_{k,021}=\frac{\begin{array}{c}-a_{k,101}G_{(2)}^{17}-a_{k,011}G_{(2)}^{27}-2a_{k,020}\left(G_{(2)}^{210}+G_{(2)}^{222}\right)-a_{k,110}\left(G_{(2)}^{110}+G_{(2)}^{122}\right)+a_{1,020}\left(H_{(2)}^{k15}+H_{(2)}^{k23}\right)\\ +a_{2,020}\left(H_{(2)}^{k20}+H_{(2)}^{k24}\right)+a_{1,011}\left(H_{(2)}^{k8}+H_{(2)}^{k12}\right)+a_{2,011}\left(H_{(2)}^{k9}+H_{(2)}^{k17}\right)+H_{(3)}^{k35}+H_{(3)}^{k47}+H_{(3)}^{k107}\end{array}}{2J_{c2}-J_{sk}}$$

$$a_{k,102}=\frac{\begin{array}{c}-2a_{k,200}G_{(2)}^{125}-a_{k,110}G_{(2)}^{225}-a_{k,101}\left(G_{(2)}^{15}+G_{(2)}^{121}\right)-a_{k,011}\left(G_{(2)}^{25}+G_{(2)}^{221}\right)+a_{1,101}\left(H_{(2)}^{k15}+H_{(2)}^{k23}\right)\\ +a_{2,101}\left(H_{(2)}^{k20}+H_{(2)}^{k24}\right)+a_{1,002}\left(H_{(2)}^{k3}+H_{(2)}^{k11}\right)+a_{2,002}\left(H_{(2)}^{k4}+H_{(2)}^{k16}\right)+H_{(3)}^{k25}+H_{(3)}^{k105}+H_{(3)}^{k121}\end{array}}{J_{c1}-J_{sk}}$$

$$a_{k,012}=\frac{\begin{array}{l}-a_{k,110}G_{(2)}^{125}-2a_{k,020}G_{(2)}^{225}-a_{k,101}\left(G_{(2)}^{110}+G_{(2)}^{122}\right)-a_{k,011}\left(G_{(2)}^{210}+G_{(2)}^{222}\right)+a_{2,011}\left(H_{(2)}^{k20}+H_{(2)}^{k24}\right)\\+a_{1,011}\left(H_{(2)}^{k15}+H_{(2)}^{k23}\right)+a_{1,002}\left(H_{(2)}^{k8}+H_{(2)}^{k12}\right)+a_{2,002}\left(H_{(2)}^{k9}+H_{(2)}^{k17}\right)+H_{(3)}^{k50}+H_{(3)}^{k110}+H_{(3)}^{k122}\end{array}}{J_{c2}-J_{sk}}$$

$$a_{k,111}=\frac{\begin{array}{l}-a_{k,101}\left(G_{(2)}^{12}+G_{(2)}^{16}\right)-a_{k,110}\left(G_{(2)}^{15}+G_{(2)}^{121}+G_{(2)}^{110}+G_{(2)}^{122}\right)-2a_{k,200}\left(G_{(2)}^{110}+G_{(2)}^{122}\right)-2a_{k,020}\left(G_{(2)}^{25}+G_{(2)}^{221}\right)\\-a_{k,011}\left(G_{(2)}^{22}+G_{(2)}^{26}\right)+a_{1,110}\left(H_{(2)}^{k15}+H_{(2)}^{k23}\right)+a_{2,110}\left(H_{(2)}^{k20}+H_{(2)}^{k24}\right)+a_{1,101}\left(H_{(2)}^{k8}+H_{(2)}^{k12}\right)+H_{(3)}^{k10}+H_{(3)}^{k22}\\+a_{2,101}\left(H_{(2)}^{k9}+H_{(2)}^{k17}\right)+a_{1,011}\left(H_{(2)}^{k3}+H_{(2)}^{k11}\right)+a_{2,011}\left(H_{(2)}^{k4}+H_{(2)}^{k16}\right)+H_{(3)}^{k30}+H_{(3)}^{k46}+H_{(3)}^{k102}+H_{(3)}^{k106}\end{array}}{J_{c1}+J_{c2}-J_{sk}}$$

$$a_{k,003}=\frac{a_{k,102}G_{(2)}^{125}+a_{k,012}G_{(2)}^{225}-a_{1,002}\left(H_{(2)}^{115}+H_{(2)}^{123}\right)-a_{2,002}\left(G_{(2)}^{220}+G_{(2)}^{224}\right)-H_{(3)}^{k125}}{J_{sk}} \tag{50}$$

For $k=1,2$. k defines the k^{th} degree-of-freedom of stable variables. J_{c1} and J_{c2} are the first and second terms of the diagonal matrix $\mathbf{J_c}$ as defined in equation (44), respectively. J_{sk} is the k^{th} term of the diagonal matrix $\mathbf{J_s}$ as defined in equation (44). $H_{(2)}^{ki}$ and $H_{(3)}^{ki}$ defined the terms of the k^{th}-line and i^{th}-column of the matrix defined by $\mathbf{H_2}$ and $\mathbf{H_3}$, respectively. $G_{(2)}^{ki}$ defined the term of the k^{th}-line and i^{th}-column of the matrix defined by $\mathbf{G_2}$.

Now, one notes that the expression of stable variables in power series in $(\mathbf{v_c},\hat{\mu})$, using a third-order polynomial approximation, uses a part of quadratic non-linear terms of center variables on the left side of equation (42) contained in $\mathbf{G_2}$. Moreover cubic terms of center variables contained in $\mathbf{H_3}$ and quadratic terms of stable variables contained in $\mathbf{H_2}$, on the right side of equation (34), appear. Then the third-order polynomial approximation allows a better approximation than the second-order polynomial approximation, with a participation of most non-linear terms in the determination of coefficients $a_{k,ijl}$. Furthermore, the determination of third-order polynomial approximation in equation (48) used the values of second-order polynomial approximation.

7.3 FOURTH-ORDER AND HIGHER ORDER SOLUTIONS

If the third-order polynomial approximation is not available, one has to use higher order polynomial approximation. The determination of coefficients $a_{k,ijl}$ for higher order is exactly the same than the determination for second and third-order forms. The expressions of the stable variables $\mathbf{v_s}=\mathbf{h}(\mathbf{v_c},\hat{\mu})$ as a power series in $(\mathbf{v_c},\hat{\mu})$ of degree 4 and 5, without constant and linear terms, are defined in equation (41). Moreover, the more the higher-order terms are used in order to express the stable variables as a power series of center variables, the more the non-linear terms appear in equation (42) for the determination of coefficients $a_{k,ijl}$.

In this section, one has shown how to determine the exact values of coefficients $a_{k,ijl}$ for a strong non-linear system with many degree of freedoms. As one has emphasised, the determination of coefficients $a_{k,ijl}$ can be obtained order by order, no recalculation of lower-order for a new evaluation of polynomial approximation $\mathbf{v_s}=\mathbf{h}(\mathbf{v_c},\hat{\mu})$ using higher order having to be performed. One has determined an analytical expression for the coefficients of second-order and third-order polynomial approximation of $\mathbf{v_s}=\mathbf{h}(\mathbf{v_c},\hat{\mu})$.

As explained previously, after the determination of the local center manifold $\mathbf{v_s}=\mathbf{h}(\mathbf{v_c},\hat{\mu})$, the dynamics restricted to the center manifold is also defined by the system (43).

8 LIMIT CYCLES

Now, one describes the procedure to obtain limit cycles for parameter values near the bifurcation point $\mu = \mu_0 + \overline{\mu}$ where μ_0 is the bifurcation point and $\overline{\mu} = \varepsilon.\mu_0$ (with $\varepsilon << 1$).

An application of the center manifold to system (26) augmented with the equation $\dot{\overline{\mu}} = 0$, shows that if the equilibrium is preserved, then the dynamics is given by equation (43). The local center manifold is represented by the polynomial expansion $\mathbf{v_s} = \mathbf{h}(\mathbf{v_c}, \overline{\mu})$ as defined previously. One notes that this method of determination of the limit cycles is a simple extension to the center manifold method, which is useful when dealing with parameterised families of systems.

In this study, one will obtain the limit cycles only near the Hopf bifurcation point (with ε very small). In this case, one observes numerically that the expressions of $\mathbf{v_s} = \mathbf{h}(\mathbf{v_c}, \overline{\mu})$ can be approximated by the expression of $\mathbf{v_s} = \mathbf{h}(\mathbf{v_c})$ with negligible errors. This approximation amounts to the expression of $\mathbf{v_s}$ at the Hopf bifurcation point μ_0 ($\mathbf{a_{ijl}} \equiv \mathbf{0}$ for $l \neq 0$). It is not necessary but nevertheless it allows the simplification of the expression of $\mathbf{v_s}$. Therefore, the non-linear terms are approximated by their evaluation at the bifurcation point $\mu = \mu_0$, provided that none of the leading nonlinear terms vanish here; so the approximation $\mathbf{G_2}[\mathbf{v_c}, \mathbf{h}(\mathbf{v_c}), \mu_0]$ and $\mathbf{G_3}[\mathbf{v_c}, \mathbf{h}(\mathbf{v_c}), \mu_0]$ are equivalent to $\mathbf{G_2}[\mathbf{v_c}, \mathbf{h}(\mathbf{v_c}), \mu]$ and $\mathbf{G_3}[\mathbf{v_c}, \mathbf{h}(\mathbf{v_c}), \mu]$ with negligible error due to the fact that ε is very small.

Finally, the dynamics of the system is described, with small errors, by the system

$$\begin{cases} \dot{\mathbf{v}}_\mathbf{c} = \mathbf{J_c}(\mu).\mathbf{v_c} + \mathbf{G_2}[\mathbf{v_c}, \mathbf{h}(\mathbf{v_c}), \mu_0] + \mathbf{G_3}[\mathbf{v_c}, \mathbf{h}(\mathbf{v_c}), \mu_0] \\ \dot{\mu} = 0 \end{cases} \tag{51}$$

This reduced system is easier to study than the original one. Using an approximation of $\mathbf{h}$ of order 2 causes divergence in the evolutions of limit cycle amplitudes. This problem is due to the fact that a polynomial approximation of $\mathbf{h}$ of order 2 is not sufficient. Then, one determines the limit cycles of the system by using an approximation of $\mathbf{h}$ of order 3.

This study uses the base parameters defined previously and the determination of the coefficients of the polynomial approximation of $\mathbf{h}$ of order 3. As previously defined, the Hopf bifurcation point is detected for $\mu_0 = 0{,}2$.

Figure 13 : X-limit cycle for $\overline{\mu} = \mu_0 / 1000$

Figure 14 : Y-limit cycle for $\overline{\mu} = \mu_0 / 1000$

In Figure 13 and Figure 14, limit cycles are plotted for the two degree-of-freedom of the physical system (4). Thin lines and star lines show limit cycle by integrating the original system and by using center manifold approach, respectively. One notices a good correlation between the integrated system and the center manifold approach by using an approximation of $\mathbf{h}$ of order 3. Consequently, the center manifold approach is validated and reduces the number of equations of the original system in order to obtain a simplified system, without losing the dynamics of the original system as well as the non-linear terms.

Now, it will be very interesting to determine the influence of varying parameters on the level amplitude. So, it is necessary to use an approximation of $\mathbf{h}$ of order 5 in some cases, since an approximation of $\mathbf{h}$ of order 3 or 4 is not enough.

For each simulation, the Hopf bifurcation point and the value of brake friction coefficient μ_0 are detected as defined in Table 1.

Table 1 : Values of brake friction coefficient at the Hopf bifurcation

Figure 15 : X-limit cycle and Y-limit cycle for $\overline{\mu} = \mu_0 / 1000$ as a function of angle θ

Figure 16 : X-limit cycle and Y-limit cycle for $\overline{\mu} = \mu_0 / 1000$ as a function of non-linear stiffness

Figure 17 : X-limit cycle and Y-limit cycle for $\overline{\mu} = \mu_0 / 1000$ as a function of brake force

Figure 18 : X-limit cycle and Y-limit cycle for $\overline{\mu} = \mu_0 / 1000$ as a function of mass m_1

Some indications have been observed by varying one parameter for the base values defined previously. It may be noted that the limit cycle is defined near the Hopf bifurcation point, using the brake friction coefficient as unfolding parameter. It is observed that the level amplitude is a very complex problem. Indeed, the evolution of limit cycle amplitude is not linear with the evolution of specific parameter. The increasing or decreasing level amplitude versus linear evolution of a specific parameter is observed. This is further reflected in Figure 15, Figure 16, Figure 17 and Figure 18.

More precisely, the growth of limit cycle amplitudes is controlled by the rise and fall of the non-linear stiffness k_{12}, as illustrated in Figure 16. Yet, the evolution of limit cycle does not decrease in the same proportion as the non-linear stiffness k_{12} increases. The evolution is not linear and the Y-limit cycle grows with changing in form.

Moreover, limit cycles increase and decrease with constant increasing of mass m_1, constant increasing of the angle θ, or constant increasing of the brake force F_{brake}, as shown in Figure 15, Figure 17 and Figure 18, respectively. The X-limit cycle evolution and Y-limit cycle evolution have not the same behaviour, and for example, Y-limit cycle grows with changing in form in Figure 15.

In conclusion, parametric studies of the evolution of limit cycles are a complex problem. Parametric design studies show that evolution of limit cycle amplitude can be altered by changes in the brake friction coefficient, brake force, stiffness, mass and angle.

9 SUMMARY AND CONCLUSION

A non-linear model for the analysis of mode heavy truck judder has been developed. Results from stability are investigated by calculating the Jacobian of the system at the equilibrium points. This stability analysis indicates that system instability can occur with a constant friction coefficient. The correlation between experiments and theoretical coupled frequencies is sufficiently satisfactory to justify the theoretical approach adopted and particularly the sprag-slip phenomena. For further understanding of the effects due to the variation of some parameters, stability analysis using two parameter evolutions has been realised. Indeed, changes in masses, stiffness, brake friction coefficient, damping and angle of the sprag-slip phenomena are significant on stability.

Moreover, this paper presents the centre manifold approach in order to obtain equations for the limit cycle amplitude. This approach simplifies the dynamics on the centre manifold by reducing the order of the dynamical system, while retaining the essential features of the dynamic behaviour near the Hop bifurcation point. One of the most important points is the determination of polynomial approximations and of power that defines expressions of stable variables versus centre manifold. The center manifold theory for this non-linear model is validated by comparing results obtained by solving the full system and by using the center manifold approach.

Finally, a particular observation is the need to determine the instability amplitude obtained by using the center manifold approach, and not only the instability region obtained by calculating the Jacobian of the system at the equilibrium points. In order to relate the effect of specific parameter variations on the stability and on the evolution of limit cycle amplitude to the design features of brake system, it is necessary to perform a complex nonlinear analysis without neglecting the study of evolution amplitude. In these cases, the center manifold approach is very interesting when time history response solutions of the full set of non-linear equations are time consuming to perform and when extensive parametric design studies are necessary.

ACKNOWLEDGMENTS

The authors gratefully acknowledge the French Education Ministry for its support through grant n°99071 for the investigation presented here.

REFERENCE

1. A.H. Nayfeh and D.T. Mook 1979 *John Wiley & Sons*. Nonlinear Oscillations.
2. A.H. Nayfeh and B. Balachandran, 1995 *John Wiley & Sons.* Applied Nonlinear Dynamics : Analytical, Comptational and Experimental Methods.
3. A.D. Brjuno, *Transactions of the Moscow Mathematical Society, 25,* 132-198. Analytical forms of differential equations, I.
4. A.D. Brjuno, Transactions of the Moscow Mathematical Society, 25, 199-299. Analytical forms of differential equations, II.
5. J. Guckenheimer and P. Holmes 1986 *Springer-Verlag* Nonlinear Oscillations, Dynamical Systems, and Bifurcations of vector Fields.
6. L. Jezequel and C.H. Lamarque 1991 *Journal of Sound and Vibration,* 149, 429-459. Analysis of Non-linear Dynamical Systems by the Normal Form Theory.
7. C. Elphick, E. Tiraipegui, M.E. Brochet, P. Couillet, G. Iooss 1986 *Phys.D, Preprint n°109, Université de Nice*. A simple global Characterization for Normal Forms of Singular vector Fields.
8. G. Iooss and D.D. Joseph 1980 *Springer-Verlag,* Elementary Bifurcation and Stability Theory.
9. L. Hsu 1983 *Journal of Sound and Vibration,* 89, 169-181. Analysis of critical and post-critical behaviour of non-linear dynamical systems by the normal form method, part I : Normalisation formulae.
10. L. Hsu 1983 *Journal of Sound and Vibration,* 89, 183-194. Analysis of critical and post-critical behaviour of non-linear dynamical systems by the normal form method, part II : Divergence and flutter.
11. P. Yu 1998 *Journal of Sound and Vibration,* 211, 19-38. Computation of normal forms via a perturbation tehcnique.
12. J.E. Marsden and M. McCracken 1976 *Spring-Verlag, Applied Mathematical Sciences 19.* The Hopf Bifurcation and its Applications.
13 E. Knobloch and K.A. Wiesenfeld 1983 *Journal of Statistical Physics,* 33, n°3. Bifurcation in Fluctuating Systems : The Center Manifold Approach.
14. M.R. North 1972 *14th FISITA congress,* Paper 1/9. A Mechanism of disc brake squeal.
15. S.W.E Earles and G.B. Soar 1971 *Proc.I.Mech.E.Conf. on "Vibration and Noise in Motor Vehicles",* Paper C100/71. Squeal noise in disc brakes.
16. N. Millner 1978 *SAE* Paper 780332. An Analysis of Disc Brake Squeal.
17. S.Y. Liu, M.A. Ozbek and J.T. Gordon 1996 *ASME Design Engineering Technical Conferences*, 3. A Nonlinear Model for Aircraft Brake Squeal Analysis. Part i : Model Description and Solution Methodology.
18. M.J. Rudd 1976 *Journal of Sound and Vibration*, 46, n°3, 381-394. Wheel/Rail Noise – Part II: Wheel Squeal.
19. M. Nakai and M. Yokoi 1996 *Journal of Vibration and Acoustics,* 118, 190-197. Band Brake Squeal.
20. R.P. Jarvis and B.Mills 1963/1964 *Proc. Instn. Mech. Engrs,* 178, n°32, 847-866. Vibrations induced by dry friction.
21. S.W.E Earles and C.K. Lee 1976 *Trans ASME, J. Engng Ind.,* 98, Series B, n°1, 81-86. Instabilities arising from the frictional interaction of a pin-disc system resulting in noise generation.
22. R.T. Spurr 1961/1962 *Proc. Auto. Div., Instn. Mech. Engrs*, n°1, 33-40. A theory of brake squeal.

23. R.A. Ibrahim 1994 *ASME Applied Mechanics Review*, 47, n°7, 209-226. Friction-Induced Vibration, Chatter, Squeal and Chaos : Part I - Mechanics of Contact and Friction.
24. R.A. Ibrahim 1994 *ASME Applied Mechanics Review*, 47, n°7, 227-253. Friction-Induced Vibration, Chatter, Squeal and Chaos : Part II – Dynamics and Modeling.
25. J.T. Oden and J.A.C Martins 1985 *Computer Methods in Apllied Mechanics and Engineering*, 52, 527-634. Models and Computational Methods for Dynamic friction Phenomena.
26. D.A. Crolla and A.M. Lang 1991 *Tribologie,* 18, Vehicle Tribology, 165-174.Brake Noise and Vibration – State of Art.
27. H.R. Mills 1938/1939 *Research Report n°9000B and Research Report n°9162B of the Institution of Automobile Engineers. Brake Squeal*.
28. A.H. Dweib and A.F. D'Souza 1990 *Journal of Sound and Vibration,* 137, 177-190. Self-excited vibrations induced by dry friction, Part 2 : Stability And Limit-Cycle Analysis.
29. H. Larsson and K. Fahrang 1997 *ASME Design Engineering Technical Conferences* DETC97/VIB-4162. Investigation of Stick-Slip Phenomenon using a Two-disk Friction System Vibration Mode.
30. S.S. Antoniou, A. Cameron and C.R. Gentle 1976 *Wear*, 36, 235-254. The Friction-speed Relation from Stick-Slip Data.
31. R.J. Black 1995 *ASME Design Engineering Technical Conferences*, 3. Self Excited Multi-mode Vibrations of Aircraft Brakes with Nonlinear Negative.
32. C. Gao, D. Kuhlmann-Wilsdorf and D.D. Makel 1994 *Wear*, 173, 1-12. The Dynamic Analysis of Stick-Slip.
33. J.P. Boudot 1995 *Thèse de Doctorat, Ecole Centrale de Lyon.* Modélisation des bruits de freinage des véhicules Industriels.
34. P. Chambrette 1991 *Thèse de Doctorat, Ecole Centrale* de Lyon. Stabilité des Systèmes Dynamiques avec Frottement sec : Application au Crissement des freins à disque.
35. F. Moirot 1998 *Thèse de Doctorat, Ecole Polytechnique*. Etude de la stabilité d'un Equilibre en Présence de Frottement de Coulomb. Application à l'Etude des Freins à Disque.
36. M. Kusano, H. Ishidou, S. Matsumura and S. Washizu *SAE,* Paper 851465. Experimental Study on the Reduction of drum Brake Noise.
37. A.M. Lang and T.P. Newcomb 1989 Paper C382/051, I.*Mech.E/EAEC Conf*., Strasbourg, Paper C382/051, An experimental investigation into drum brake squeal.
38. S.W.E Earles and P.W. Chambers 1987 *Int. J. of vehicle Design*, 8, nos 4/5/6, 538-552.Disc Brake Squeal Noise generation : Predicting its Dependency on System parameters Including Damping.
39. A.F. D'Souza. 1988 *Design of Control Systems.* Englewood Cliffs, New Jersey: Pretice-Hall, pp. 190-203.
40. G.W. Stewart and Ji-guang Sun 1990 *Academic Press.* Computer Science and Scientific Computing. Matrix Perturbation Theory.
41. J. Carr 1981 *Springer-Verlag.* Application of Center Manifold.

APPENDIX A : PARAMETER VALUES

$F_{brake} = 1N$	brake force
$m_1 = 1kg$	equivalent mass of first mode
$m_2 = 1kg$	equivalent mass of second mode
$c_1 = 5N/m/sec$	equivalent damping of first mode
$c_2 = 5N/m/sec$	equivalent damping of second mode
$k_{11} = 1.10^5 N/m$	coefficient of linear term of stiffness k_1
$k_{12} = 1.10^6 N/m^2$	coefficient of quadratic term of stiffness k_1
$k_{13} = 1.10^6 N/m^3$	coefficient of cubic term of stiffness k_1
$k_{21} = 1.10^5 N/m$	coefficient of linear term of stiffness k_2
$k_{22} = 1.10^5 N/m^2$	coefficient of quadratic term of stiffness k_2
$k_{23} = 1.10^5 N/m^3$	coefficient of cubic term of stiffness k_2
$\theta = 0{,}2rad$	sprag-slip angle
$\mu = 0{,}3$	brake friction coefficient

APPENDIX B : JACOBIAN MATRIX AND EXPRESSIONS OF a_3, a_2, a_1 AND a_0

The terms of the Jacobian matrix $\mathbf{J}$ of the system at the equilibrium points $\mathbf{x_0} = \{X_0 \;\; Y_0\}^{\mathrm{T}}$, are :

$$\mathbf{J}(1,1) = \mathbf{J}(1,2) = \mathbf{J}(1,4) = \mathbf{J}(2,1) = \mathbf{J}(2,2) = \mathbf{J}(2,3) = 0 \;\; ; \qquad \mathbf{J}(1,3) = \mathbf{J}(2,4) = 1$$

$$\mathbf{J}(3,1) = \frac{-1}{m_2\left(\tan^2\theta+1\right)\left(k_{21}\left(1+\mu\tan\theta\right)+k_{11}\left(\tan^2\theta-\mu\tan\theta\right)-\left(-\tan\theta+\mu\right)\left(2k_{12}\tan^2\theta.X_0-2k_{12}\tan\theta.Y_0\right.\right.}$$
$$\left.\left.+3k_{13}\tan^3\theta.{X_0}^2-6k_{13}\tan^2\theta.X_0.Y_0+3k_{13}\tan\theta.{Y_0}^2\right)+\left(1+\mu\tan\theta\right)\left(2k_{22}.X_0+3k_{23}.{X_0}^2\right)\right)$$

$$\mathbf{J}(3,2) = \frac{-1}{m_2\left(\tan^2\theta+1\right)\left(k_{11}\left(-\tan\theta+\mu\right)-\left(-\tan\theta+\mu\right)\left(2k_{12}.Y_0-2k_{12}\tan\theta.X_0-3k_{13}\tan^2\theta.{X_0}^2+6k_{13}\tan\theta.X_0.Y_0-3k_{13}.{Y_0}^2\right)\right)}$$

$$\mathbf{J}(3,3) = \frac{-c_1\left(\tan^2\theta-\mu\tan\theta\right)+c_2\left(1+\mu\tan\theta\right)}{m_2\left(\tan^2\theta+1\right)}$$

$$\mathbf{J}(3,4) = \frac{c_1\left(\tan\theta-\mu\right)}{m_2\left(\tan^2\theta+1\right)}$$

$$\mathbf{J}(4,1) = \frac{-1}{m_1\left(-k_{11}\tan\theta+2k_{12}\tan^2\theta.X_0-2k_{12}\tan\theta.Y_0-3k_{13}\tan\theta.{Y_0}^2+6k_{13}\tan^2\theta.X_0.Y-3k_{13}\tan^3\theta.{X_0}^2\right)}$$

$$\mathbf{J}(4,2) = \frac{-1}{m_1\left(k_{11}+2k_{12}.Y_0-2k_{12}\tan\theta.X_0+3k_{13}.{Y_0}^2-6k_{13}\tan\theta.X_0.Y_0+3k_{13}\tan^2\theta.{X_0}^2\right)}$$

$$\mathbf{J}(4,3)=\frac{c_1\tan\theta}{m_1} \quad ; \quad \mathbf{J}(4,4)=\frac{-c_1}{m_1}$$

The expressions of a_3, a_2, a_1 and a_0 are

$$a_3=\frac{c_1\left(\tan^2\theta-\mu\tan\theta\right)+c_2\left(1+\mu\tan\theta\right)}{m_2\left(\tan^2\theta+1\right)}+\frac{c_1}{m_1}$$

$$a_2=\frac{k_{11}+2k_{12}.Y_0-2k_{12}\tan\theta.X_0+3k_{13}.Y_0^{\,2}-6k_{13}\tan\theta.X_0.Y_0+3k_{13}\tan^2\theta.X_0^{\,2}}{m_1}+\frac{c_1c_2\left(1+\mu\tan\theta\right)}{m_1m_2\left(\tan^2\theta+1\right)}$$
$$+\frac{\begin{array}{l}k_{21}\left(1+\mu\tan\theta\right)+k_{11}\left(\tan^2\theta-\mu\tan\theta\right)-\left(-\tan\theta+\mu\right)\left(2k_{12}\tan^2\theta.X_0-2k_{12}\tan\theta.Y_0\right.\\\left.+3k_{13}\tan^3\theta.X_0^{\,2}-6k_{13}\tan^2\theta.X_0.Y_0+3k_{13}\tan\theta.Y_0^{\,2}\right)+\left(1+\mu\tan\theta\right)\left(2k_{22}.X_0+3k_{23}.X_0^{\,2}\right)\end{array}}{m_2\left(\tan^2\theta+1\right)}$$

$$a_1=\frac{\begin{array}{l}c_1\left(k_{21}\left(1+\mu\tan\theta\right)+k_{11}\left(\tan^2\theta-\mu\tan\theta\right)-\left(-\tan\theta+\mu\right)\left(2k_{12}\tan^2\theta.X_0-2k_{12}\tan\theta.Y_0\right.\right.\\\left.+3k_{13}\tan^3\theta.X_0^{\,2}-6k_{13}\tan^2\theta.X_0.Y_0+3k_{13}\tan\theta.Y_0^{\,2}\right)+\left(1+\mu\tan\theta\right)\left(2k_{22}.X_0+3k_{23}.X_0^{\,2}\right)\Big)\\+c_1\left(\tan\theta-\mu\right)\left(-k_{11}\tan\theta+2k_{12}\tan^2\theta.X_0-2k_{12}\tan\theta.Y_0-3k_{13}\tan\theta.Y_0^{\,2}+6k_{13}\tan^2\theta.X_0.Y-3k_{13}\tan^3\theta.X_0^{\,2}\right)\\+c_1\tan\theta\left(k_{11}\left(-\tan\theta+\mu\right)-\left(-\tan\theta+\mu\right)\left(2k_{12}.Y_0-2k_{12}\tan\theta.X_0-3k_{13}\tan^2\theta.X_0^{\,2}+6k_{13}\tan\theta.X_0.Y_0-3k_{13}.Y_0^{\,2}\right)\right)\\+\left(c_1\left(\tan^2\theta-\mu\tan\theta\right)+c_2\left(1+\mu\tan\theta\right)\right)\left(k_{11}+2k_{12}.Y_0-2k_{12}\tan\theta.X_0+3k_{13}.Y_0^{\,2}-6k_{13}\tan\theta.X_0.Y_0+3k_{13}\tan^2\theta.X_0^{\,2}\right)\end{array}}{m_1m_2\left(\tan^2\theta+1\right)}$$

$$a_0=\frac{\begin{array}{l}\left(k_{21}\left(1+\mu\tan\theta\right)+k_{11}\left(\tan^2\theta-\mu\tan\theta\right)-\left(-\tan\theta+\mu\right)\left(2k_{12}\tan^2\theta.X_0-2k_{12}\tan\theta.Y_0\right.\right.\\\left.+3k_{13}\tan^3\theta.X_0^{\,2}-6k_{13}\tan^2\theta.X_0.Y_0+3k_{13}\tan\theta.Y_0^{\,2}\right)+\left(1+\mu\tan\theta\right)\left(2k_{22}.X_0+3k_{23}.X_0^{\,2}\right)\Big)\\\times\left(k_{11}+2k_{12}.Y_0-2k_{12}\tan\theta.X_0+3k_{13}.Y_0^{\,2}-6k_{13}\tan\theta.X_0.Y_0+3k_{13}\tan^2\theta.X_0^{\,2}\right)\\+\left(k_{11}\tan\theta-2k_{12}\tan^2\theta.X_0+2k_{12}\tan\theta.Y_0+3k_{13}\tan\theta.Y_0^{\,2}-6k_{13}\tan^2\theta.X_0.Y+3k_{13}\tan^3\theta.X_0^{\,2}\right)\\\times\left(k_{11}\left(-\tan\theta+\mu\right)-\left(-\tan\theta+\mu\right)\left(2k_{12}.Y_0-2k_{12}\tan\theta.X_0-3k_{13}\tan^2\theta.X_0^{\,2}+6k_{13}\tan\theta.X_0.Y_0-3k_{13}.Y_0^{\,2}\right)\right)\end{array}}{m_1m_2\left(\tan^2\theta+1\right)}$$

APPENDIX C : DEFINITION OF $\mathbf{f_{(1)}^{i}}$, $\mathbf{f_{(2)}^{ij}}$ AND $\mathbf{f_{(3)}^{ijk}}$ COEFFICIENTS

The vectors $\mathbf{f_{(1)}^{i}}$, $\mathbf{f_{(2)}^{ij}}$ and $\mathbf{f_{(3)}^{ijk}}$ are coefficients of the linear, quadratic and cubic terms of the nonlinear force $\mathbf{P_{NL}} = \left\{P_{NL}^{X} \;\; P_{NL}^{Y}\right\}^{\mathrm{T}}$, respectively , due to the nonlinear stiffness about the equilibrium point. The non-zero components of the vectors $\mathbf{f_{(1)}^{i}} = \left\{f_{(1)}^{X,i} \; f_{(1)}^{Y,i}\right\}^{\mathrm{T}}$, $\mathbf{f_{(2)}^{ij}} = \left\{f_{(2)}^{X,ij} \; f_{(2)}^{Y,ij}\right\}^{\mathrm{T}}$ and $\mathbf{f_{(3)}^{ijk}} = \left\{f_{(3)}^{X,ijk} \; f_{(3)}^{Y,ijk}\right\}^{\mathrm{T}}$,respectively , are :

$$f_{(1)}^{X,1} = \left(-\tan\theta+\mu\right)\left[2k_{12}\tan^2\theta.X_0 - 2k_{12}\tan\theta.Y_0 + 3k_{13}\tan^3\theta.X_0{}^2 - 6k_{13}\tan^2\theta.X_0.Y_0 + 3k_{13}\tan\theta.Y_0{}^2\right]$$
$$+\left(1+\mu\tan\theta\right)\left[2k_{22}.X_0 + 3k_{23}.X_0{}^2\right]$$
$$f_{(1)}^{X,2} = \left(-\tan\theta+\mu\right)\left[2k_{12}.Y_0 - 2k_{12}\tan\theta.X_0 - 3k_{13}\tan^2\theta.X_0{}^2 + 6k_{13}\tan\theta.X_0.Y_0 - 3k_{13}.Y_0{}^2\right]$$

$$f_{(1)}^{Y,1} = -2k_{12}\tan^2\theta.X_0 + 2k_{12}\tan\theta.Y_0 + 3k_{13}\tan\theta.Y_0{}^2 - 6k_{13}\tan^2\theta.X_0.Y + 3k_{13}\tan^3\theta.X_0{}^2$$
$$f_{(1)}^{Y,2} = -2k_{12}.Y_0 + 2k_{12}\tan\theta.X_0 - 3k_{13}.Y_0{}^2 + 6k_{13}\tan\theta.X_0.Y_0 - 3k_{13}\tan^2\theta.X_0{}^2$$

$$f_{(2)}^{X,11} = \left(-\tan\theta+\mu\right).\left[k_{12}.\tan^2\theta + 3k_{13}.\tan^3\theta.X_0 - 3k_{13}.\tan^2\theta.Y_0\right] + \left(1+\tan\theta\right)\left[k_{22} + 3k_{23}.X_0\right]$$
$$f_{(2)}^{X,12} = \left(-\tan\theta+\mu\right).\left[-2k_{12}.\tan\theta - 6k_{13}.\tan^2\theta.X_0 + 6k_{13}.\tan\theta.Y_0\right]$$
$$f_{(2)}^{X,22} = \left(-\tan\theta+\mu\right).\left[k_{12} - 3k_{13}.\tan\theta.X_0 - 3k_{13}..Y_0\right]$$

$$f_{(2)}^{Y,11} = -k_{12}.\tan^2\theta - 3k_{13}.\tan^2\theta.Y_0 + 3k_{13}.\tan^3\theta.X_0$$
$$f_{(2)}^{Y,12} = 2k_{12}.\tan\theta + 6k_{13}.\tan\theta.Y_0 - 6k_{13}.\tan^2\theta.X_0$$
$$f_{(2)}^{Y,22} = -k_{12} - 3k_{13}.Y_0 - 3k_{13}.\tan\theta.X_0$$
$$f_{(3)}^{X,111} = \left(-\tan\theta+\mu\right).k_{13}.\tan^3\theta + k_{23}.\left(1+\tan\theta\right)$$
$$f_{(3)}^{X,112} = -3k_{13}.\tan^2\theta\left(-\tan\theta+\mu\right)$$
$$f_{(3)}^{X,122} = 3k_{13}.\tan\theta\left(-\tan\theta+\mu\right)$$
$$f_{(3)}^{X,222} = -k_{13}.\left(-\tan\theta+\mu\right)$$

$$f_{(3)}^{Y,111} = k_{13}.\tan^3\theta$$
$$f_{(3)}^{Y,112} = -3k_{13}.\tan^2\theta$$
$$f_{(3)}^{Y,122} = 3k_{13}.\tan\theta$$
$$f_{(3)}^{Y,222} = -k_{13}$$

APPENDIX D: NOMENCLATURE

x	scalar
$\mathbf{x}$	vector
$\dot{\mathbf{x}}$	vector of velocity
$\ddot{\mathbf{x}}$	vector of acceleration
$\mathbf{x_0}$	equilibrium point
$\bar{\mathbf{x}}$	small pertubation
$\mathbf{C}$	damping matrix
$\mathbf{K}$	stiffness matrix
$\mathbf{M}$	mass matrix
$\mathbf{J}$	Jacobian matrix of the system
$\mathbf{F}$	vector force
$\mathbf{P_{NL}}$	vector of linear and non-linear terms
$\mathbf{F_L}$	vector of linear terms
$\mathbf{F_{NL}}$	vector of non-linear terms
F^X	X- coordonate of the vector $\mathbf{F}$
F^Y	Y-coordonate of the vector $\mathbf{F}$
N	normal load
T	tangential load
m_1	equivalent mass of tangential mode
m_2	equivalent mass of torsional mode
k_1	equivalent stiffness of tangential mode
k_2	equivalent stiffness of torsional mode
c_1	equivalent damping of tangential mode
c_2	equivalent damping of torsional mode
k_{11}	coefficient of linear term of stiffness k_1
k_{12}	coefficient of quadratic term of stiffness k_1
k_{13}	coefficient of cubic term of stiffness k_1
k_{21}	coefficient of linear term of stiffness k_2
k_{22}	coefficient of quadratic term of stiffness k_2
k_{23}	coefficient of cubic term of stiffness k_2
θ	sprag-slip angle
μ	brake friction coefficient
μ_0	brake friction coefficient at the Hopf bifurcation point
$\mathbf{f^i_{(1)}}$	coefficients of linear terms
$\mathbf{f^{ij}_{(2)}}$	coefficients of quadratic non-linear terms
$\mathbf{f^{ijk}_{(3)}}$	coefficients of cubic non-linear terms
$\boldsymbol{\eta}^{\mathbf{ij}}_{\mathbf{(2)}}$	coefficients of quadratic non-linear terms in state variables
$\boldsymbol{\eta}^{\mathbf{ijk}}_{\mathbf{(3)}}$	coefficients of cubic non-linear terms in state variables
$\mathbf{a_{ijl}}$	vector of the coefficients of the center manifold
$a_{k,ijl}$	coefficients of the center manifold for the k^{th} stable variable
$\mathbf{v_c}$	vector of center variables
$\mathbf{v_s}$	vector of stable variables

$\mathbf{h}$	vector of the polynomial approximation of stable variables in center variables
$\mathbf{J_s}$	Jacobian matrix of stable variables
$\mathbf{J_c}$	Jacobian matrix of center variables
$\mathbf{G_2}$	vector function of quadratic terms for the center variables
$\mathbf{H_2}$	vector function of quadratic terms for the stable variables
$\mathbf{G_3}$	vector function of cubic terms for the center variables
$\mathbf{H_3}$	vector function of cubic terms for the stable variables

	Angle θ				Quadratic non-linear stiffness k_{12}			
	0.1	0.3	0.4	0.5	10^7	$1.5\ 10^7$	$2.5\ 10^7$	10^8
μ_0	0.103	0.3102	0.424	0.547	0.204	0.204	0.204	0.205
	F_{brake}				Mass m_1			
	10	50	100	200	1.1	1.2	1.3	1.4
μ_0	0.204	0.204	0.205	0.206	0.216	0.247	0.293	0.351

Table 1 : Values of brake friction coefficient at the Hopf bifurcation

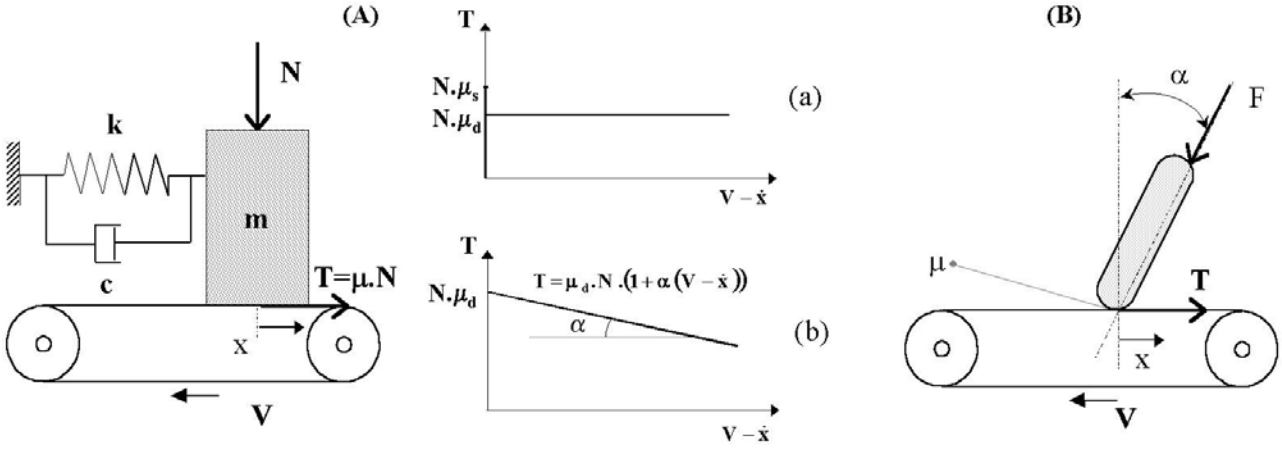

Figure 1 : Stick-slip and sprag-slip models

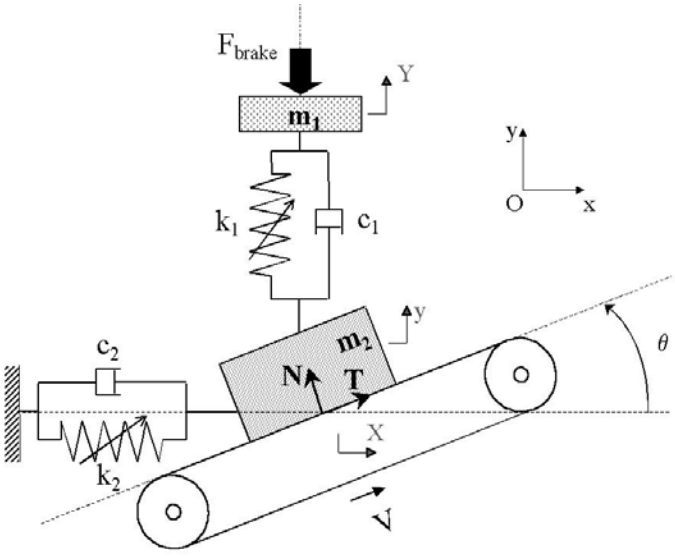

Figure 2 : Dynamic model of braking system

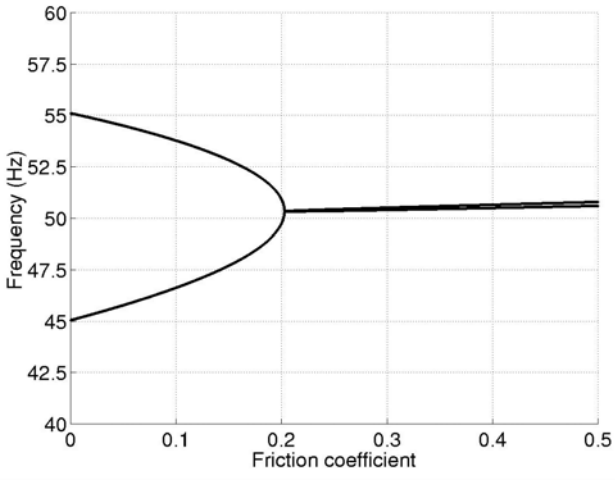

Figure 3 : Coupling of two eigenvalues

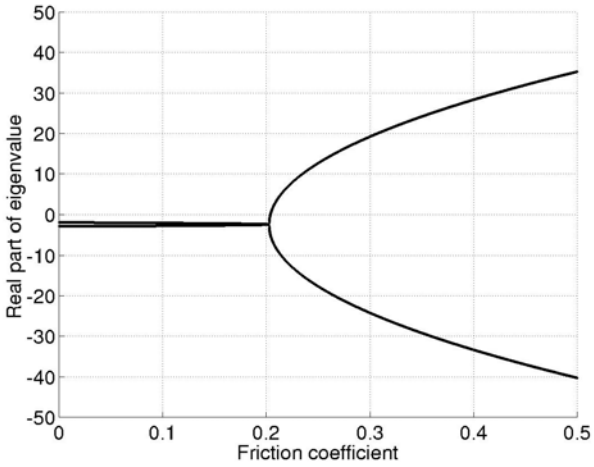

Figure 4 : Evolution of the real part of two coupling modes

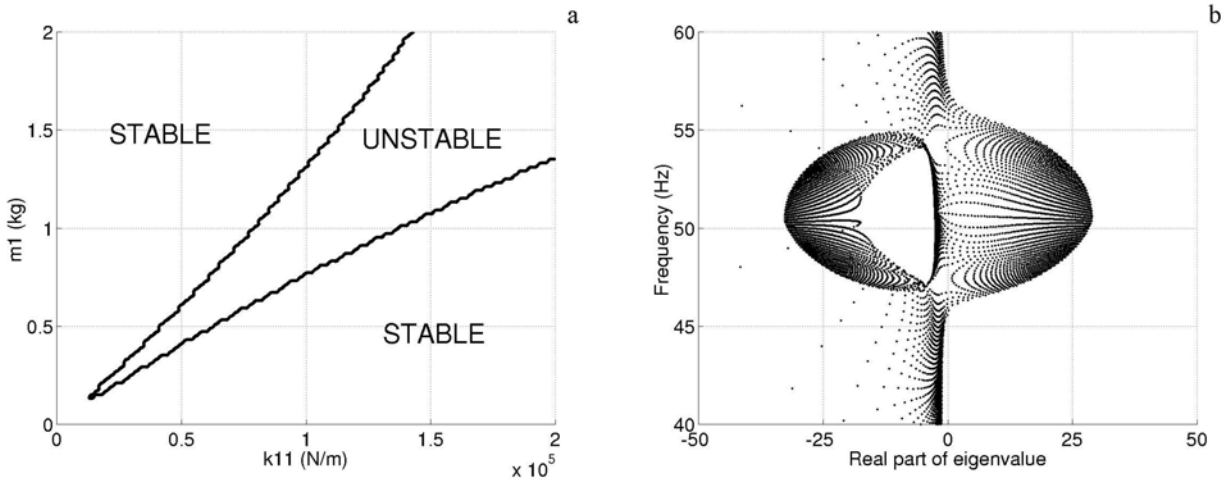

Figure 5 : Stability and complex eigenvalues as a function of mass m_1 and stiffness k_{11}. Coupled resonant frequencies between 47-57 Hz.

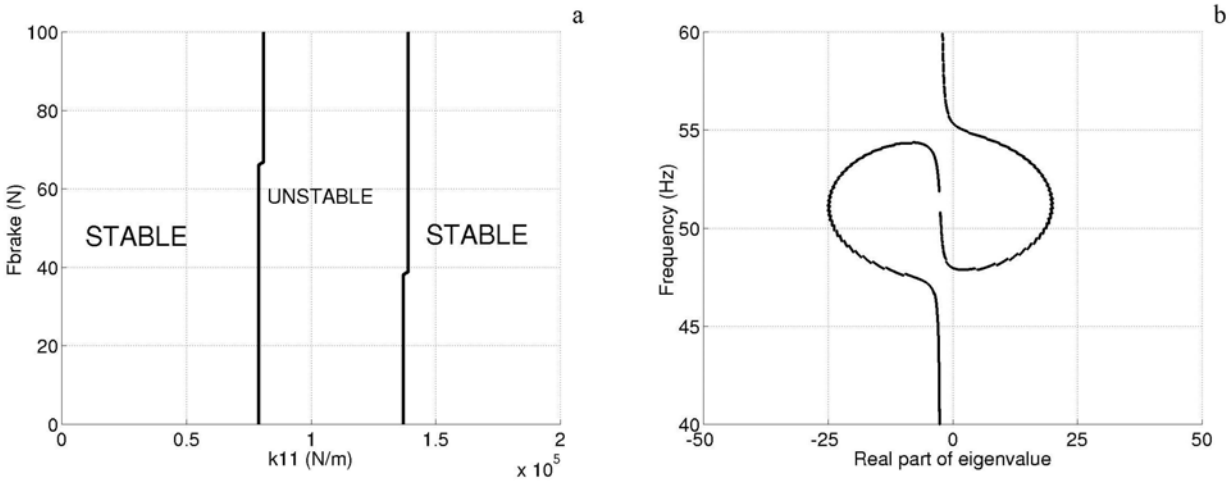

Figure 6 : Stability and complex eigenvalues as a function of force F_{brake} and stiffness k_{11}. Coupled resonant frequencies between 47-48 Hz and 55-56 Hz.

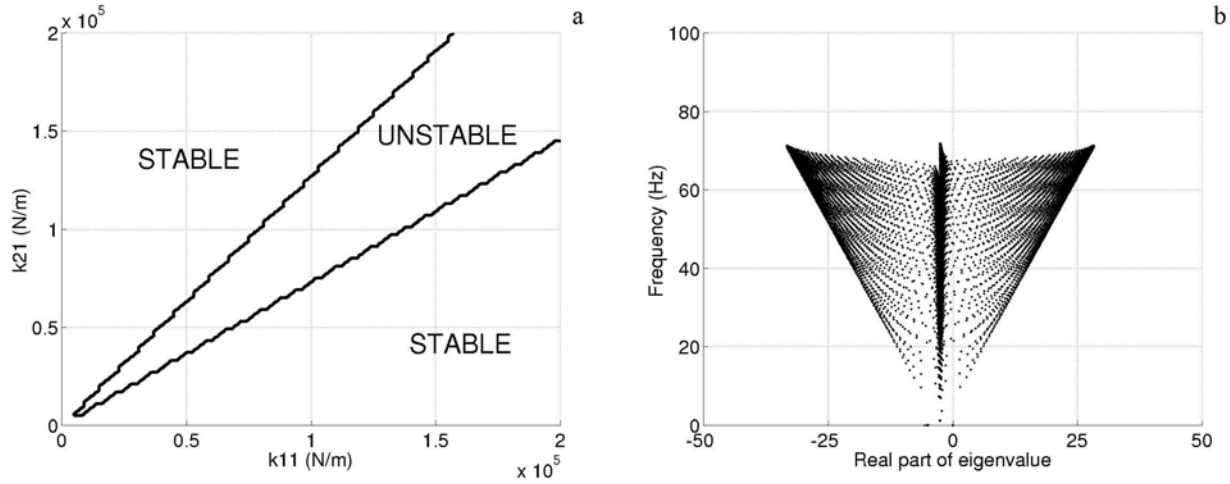

Figure 7: Stability and complex eigenvalues as a function of stiffness k_{21} and stiffness k_{11}. Coupled resonant frequencies between 10-70 Hz.

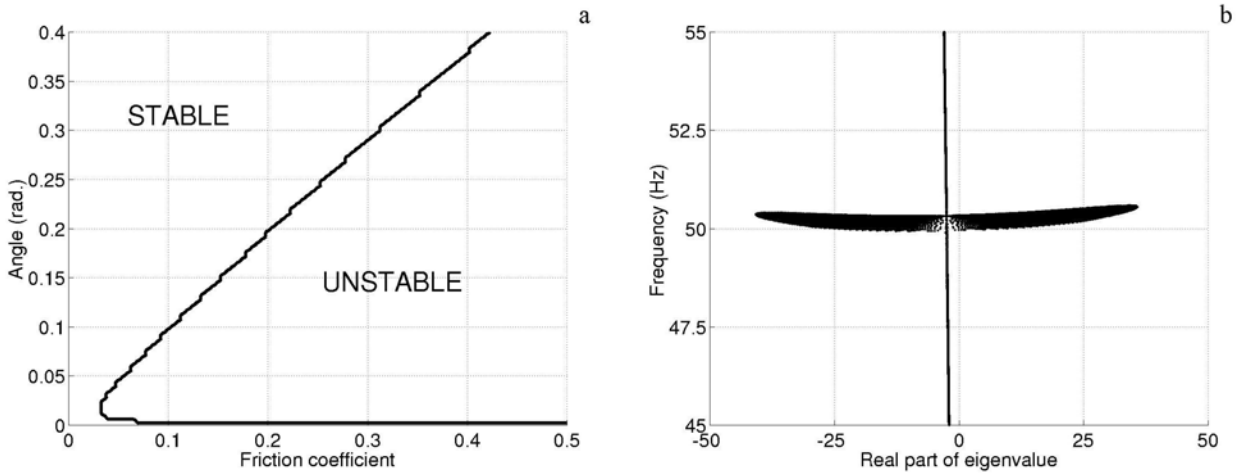

Figure 8 : Stability and complex eigenvalues as a function of angle θ and brake friction coefficient. Coupled resonant frequencies between 50-51 Hz.

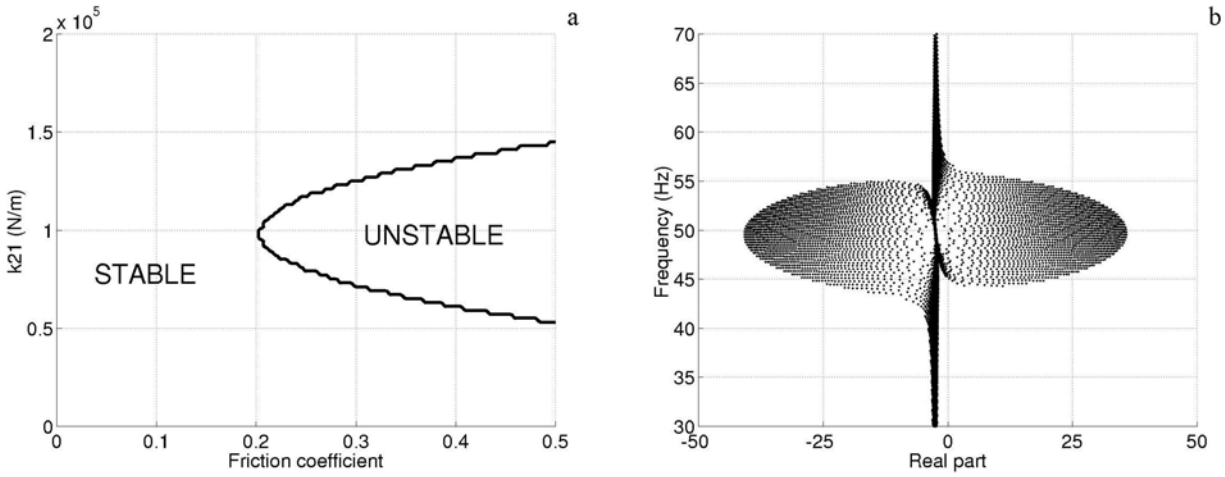

Figure 9 : Stability and complex eigenvalues as a function of stiffness k_{21} and brake friction coefficient. Coupled resonant frequencies between 45-58 Hz.

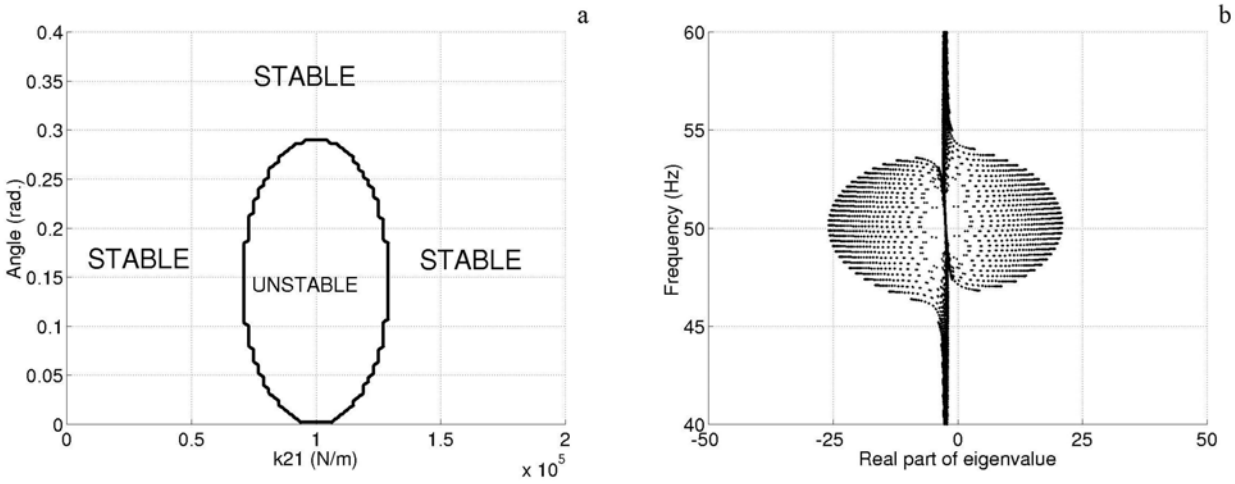

Figure 10 : Stability and complex eigenvalues as a function of angle θ and stiffness k_{21}. Coupled resonant frequencies between 47-54 Hz.

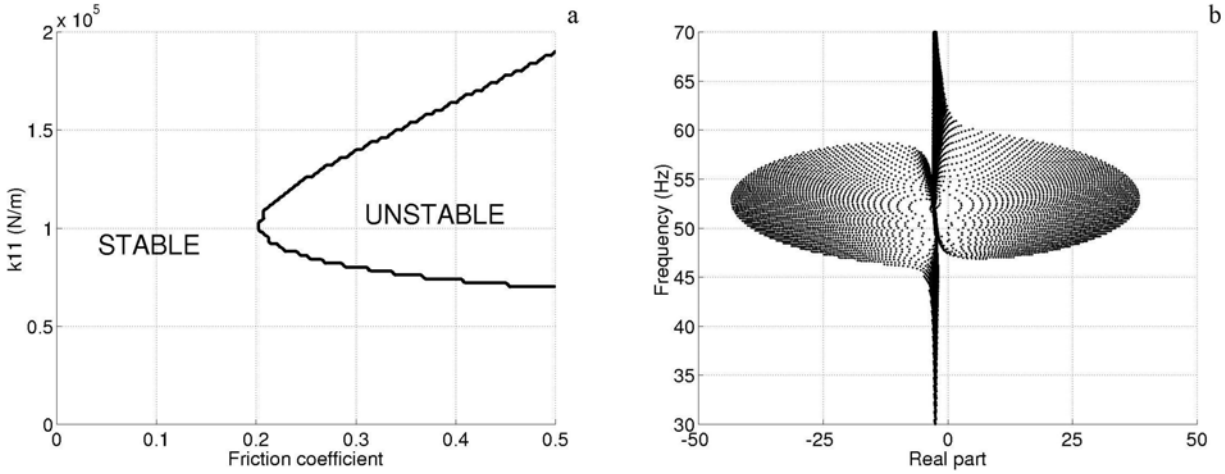

Figure 11 : Stability and complex eigenvalues as a function of stiffness k_{11} and brake friction coefficient. Coupled resonant frequencies between 48-52 Hz.

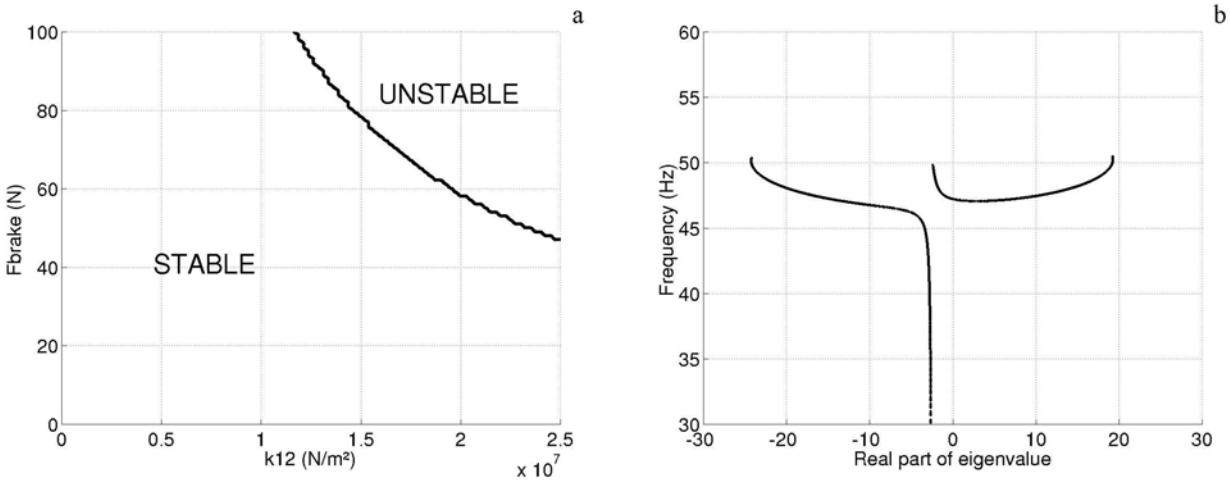

Figure 12 : Stability and complex eigenvalues as a function of stiffness k_{12} and force F_{brake}. Coupled resonant frequencies between 47-47 Hz.

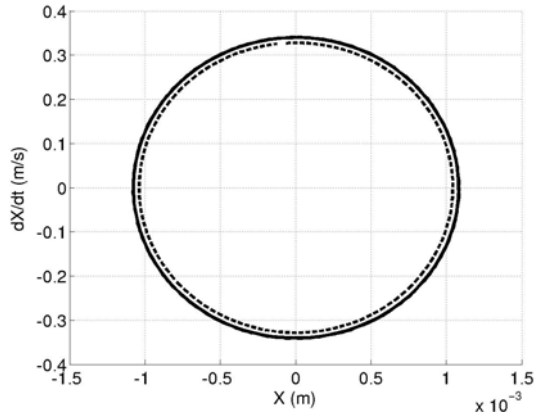

Figure 13 : X-limit cycle for $\overline{\mu} = \mu_0 / 1000$ (—— Original system, ····· Center manifold approach)

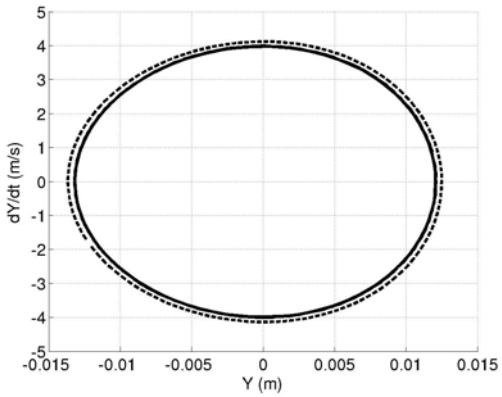

Figure 14 : Y-limit cycle for $\overline{\mu} = \mu_0 / 1000$ (—— Original system, ····· Center manifold approach)

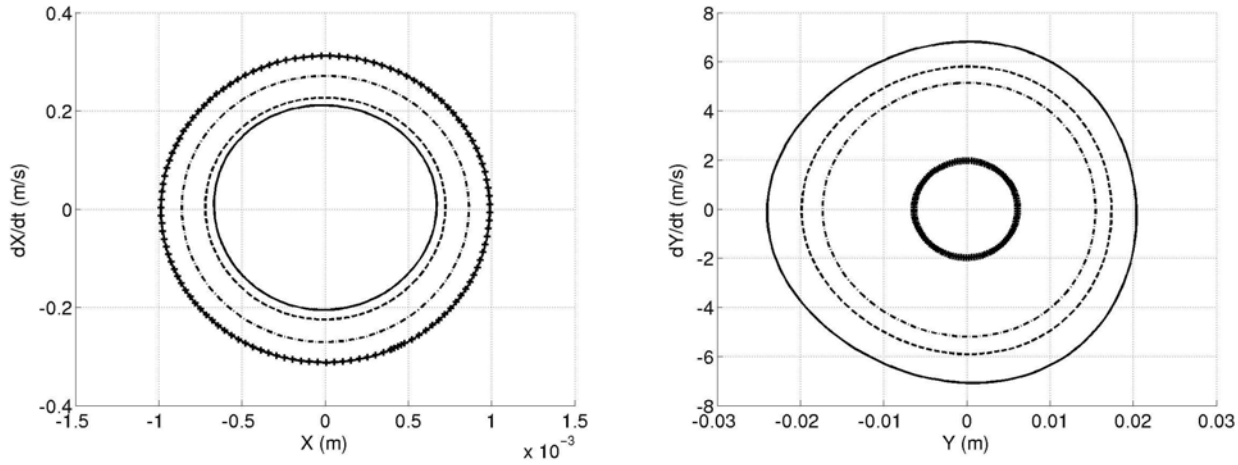

Figure 15 : X-limit cycle and Y-limit cycle for $\overline{\mu} = \mu_0 / 1000$ as a function of angle θ
(+++++ θ=0.1rad., ····· θ=0.3rad., —— θ=0.4rad., ---- θ=0.5rad)

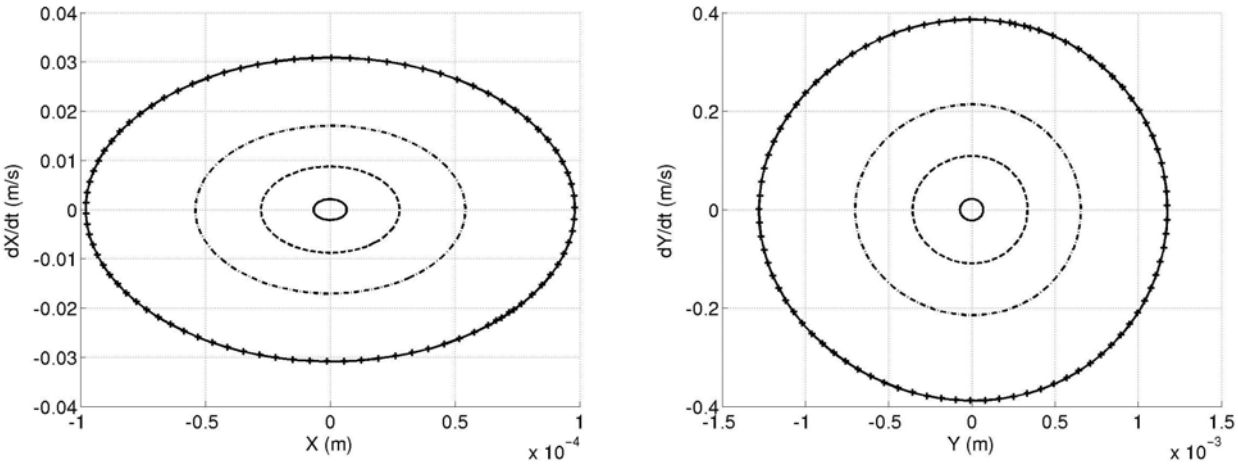

Figure 16 : X-limit cycle and Y-limit cycle for $\overline{\mu} = \mu_0 / 1000$ as a function of non-linear stiffness coefficient k_{12} (+++++ $k_{12} = 10^7 N/m^2$, ----- $k_{12} = 1.510^7 N/m^2$, ---- $k_{12} = 2.510^7 N/m^2$, —— $k_{12} = 10^8 N/m^2$)

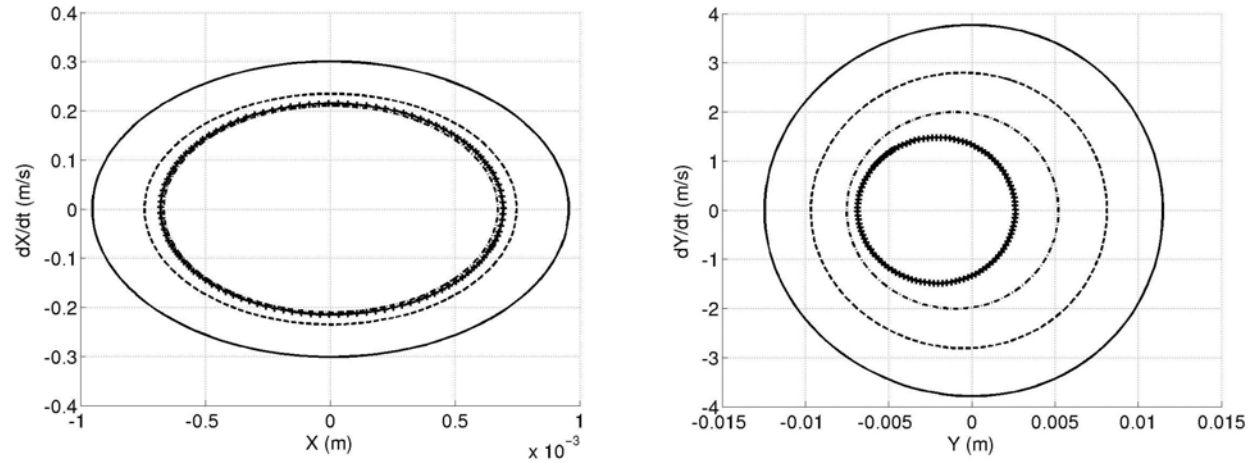

Figure 17 : X-limit cycle and Y-limit cycle for $\overline{\mu} = \mu_0 / 1000$ as a function of brake force F_{brake} (—— $F_{brake} = 10N$, ---- $F_{brake} = 10N$, ····· $F_{brake} = 10N$, +++++ $F_{brake} = 10N$).

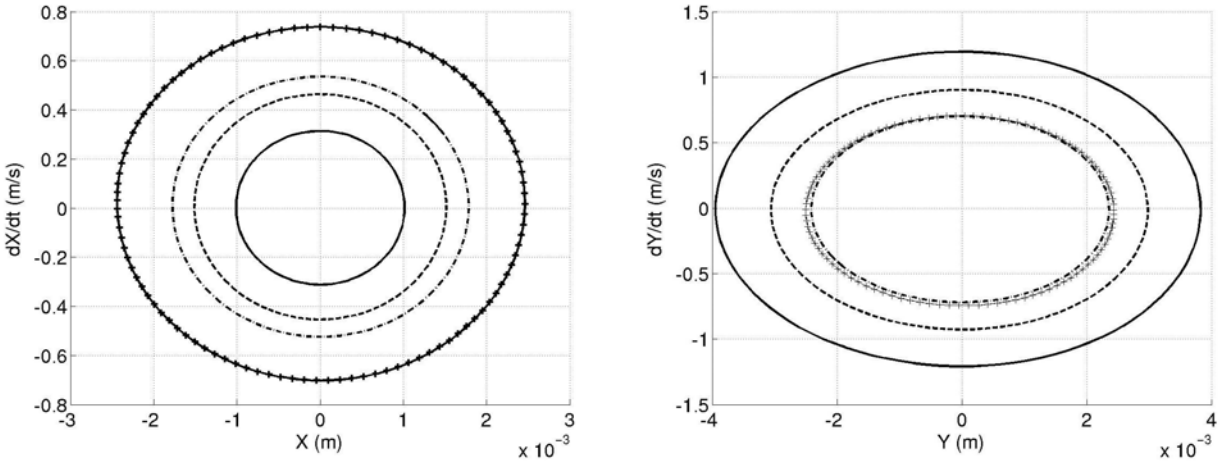

Figure 18 : X-limit cycle and Y-limit cycle for $\overline{\mu} = \mu_0 / 1000$ as a function of mass m_1 (—— $m_1 = 1.1kg$, ---- $m_1 = 1.2kg$, -·-·- $m_1 = 1.3kg$, +++++ $m_1 = 1.4kg$).